

Dissertationes Forestales 341

**Biochar as a water protection tool in peatland forestry –
nutrient recovery from runoff water**

Elham Kakaei Lafdani
School of Forest Sciences
Faculty of Science and Forestry
University of Eastern Finland

Academic dissertation

To be presented by permission of the Faculty of Science, Forestry and Technology for
public examination in the Auditorium C2 in the Karelia Building at
the University of Eastern Finland, Joensuu, on the 22th of September 2023,
at 12 o'clock noon

Title of dissertation: Biochar as a water protection tool in peatland forestry – nutrient recovery from runoff water

Author: Elham Kakaei Lafdani

Dissertationes Forestales 341

<https://doi.org/10.14214/df.341>

© Author

Licensed [CC BY-NC-ND 4.0](https://creativecommons.org/licenses/by-nc-nd/4.0/)

Thesis Supervisors:

Professor Annamari Lauren

School of Forest Sciences, University of Eastern Finland, Finland

Associate Professor Marjo Palviainen

Department of Forestry, University of Helsinki, Finland

Professor Jukka Pumpanen

Department of Environmental and Biosciences, University of Eastern Finland, Finland

Pre-examiners:

Senior Research Scientist Tuija Mattsson

Finnish Environment Institute (Syke), Helsinki, Finland

Docent, Senior Scientist Lars Högbom

Skogforsk, Uppsala, Sweden

Opponent:

Senior Research Scientist, Anna-Kaisa Ronkanen

Finnish Environment Institute (Syke), Oulu, Finland

ISSN 1795-7389 (online)

ISBN 978-951-651-772-1 (pdf)

Publishers:

Finnish Society of Forest Science

Faculty of Agriculture and Forestry of the University of Helsinki

School of Forest Sciences of the University of Eastern Finland

Editorial Office:

Finnish Society of Forest Science

Viikinkaari 6, 00790 Helsinki, Finland

<https://www.dissertationesforestales.fi>

Kakaei Lafdani E. (2023). Biochar as a water protection tool in peatland forestry – nutrient recovery from runoff water. *Dissertationes Forestales* 341. 53 p. <https://doi.org/10.14214/df.341>

ABSTRACT

Water quality is significantly affected by the forest logging activities that are carried out in drained peatlands, which causes a notable enhancement in sediment loading and nutrient export to water bodies. Furthermore, the seasonal fluctuations in nutrient concentrations in the runoff further underscore the need for efficient water protection tools in peatland forestry. To address these issues, biochar-based adsorption methods can potentially offer an effective alternative for water protection in peatland forestry.

The current thesis investigates the potential for adsorption-based nutrient recovery from clear-cut peatland runoff water using Norway spruce and Silver birch biochars. In particular, the aim is to i) study the adsorption characteristics in relation to biochar properties and nutrient compounds in runoff waters in a small-scale laboratory experiment (Paper **I**); ii) investigate the adsorption characteristics of nitrogen (N) compounds from runoff water in a meso-scale laboratory experiment that utilises biochar reactors (Paper **II**); and iii) investigate the dynamics of biochar adsorption and desorption under fluctuating total nitrogen (TN) concentrations in runoff water (Paper **III**).

Biochar made from birch and spruce were shown to efficiently adsorb N compounds from the water. Across all experiments, the TN content declined significantly, irrespective of the scale, or whether the runoff volume ranged from litres (**I** and **III**) to hundreds of litres (**II**). Furthermore, the TN content at the beginning of the experiment declined at the fastest rate. The results indicate that cases of relatively low adsorption capacity were attributed to the low initial TN concentrations in the water. In addition, TN adsorption occurs above a threshold concentration in natural runoff water. The spruce did not adsorb TN when the concentrations in the runoff water fell below 0.4 mg L^{-1} . In this thesis, biochar emerges as a compelling water protection solution, particularly in regions where clear-cut peatlands release substantial quantities of nutrients.

Keywords: adsorption rate, adsorption capacity, clear-cut, desorption, nitrogen compounds, total nitrogen

ACKNOWLEDGEMENTS

I would like to express my most sincere appreciation and gratitude to all those who have supported me throughout my journey towards completing my PhD thesis. First and foremost, I would like to extend my heartfelt thanks to my main supervisor, Annamari Laurén, whose guidance, encouragement, and unwavering support have been instrumental in helping me navigate through the challenges of my research. Her invaluable insights, constructive feedback, and constant motivation have pushed me to strive for excellence and never give up on my goals. I am also immensely grateful to my co-supervisors, Jukka Pumpanen and Marjo Palviainen, for their valuable contributions to my project. Their expertise, knowledge, guidance, and financial support have been crucial in shaping my research and helping me to overcome the obstacles I encountered along the way. I would also like to acknowledge the contributions of the lab technicians, Leena Kuusisto, Risto Ikonen, and Marja Noponen. Their attention to detail, patience, and support have been invaluable throughout my research journey. My heartfelt thanks also go out to my husband, Saleh, whose unwavering support, love, and understanding have been my constant source of strength and motivation. His encouragement, patience, and sacrifices have been crucial in enabling me to focus on my research and complete this journey. I am also grateful to my family, especially my parents, for their unconditional love and unwavering support throughout my academic journey. Their encouragement and sacrifices have enabled me to achieve my goals and pursue my dreams. Lastly, I express my sincere gratitude to the University of Eastern Finland, whose funding and support have made this project possible. Their generous support has been crucial in enabling me to pursue my research goals and contribute to the scientific community.

Joensuu, September 2023
Elham Kakaei Lafdani

LIST OF ORIGINAL ARTICLES

This thesis is based on data presented in the following articles, which are referred to in the text by the Roman numerals I-III. Articles are reproduced with the kind permission of the publishers.

- I Saarela T, Kakaei Lafdani E, Laurén A, Pumpanen J, Palviainen M. (2020). Biochar as adsorbent in purification of forest clear-cut runoff water: adsorption rate and adsorption capacity. *Biochar*, 2: 227–237. <https://doi.org/10.1007/s42773-020-00049-z>
- II Kakaei Lafdani E, Saarela T, Lauren A, Pumpanen J, Palviainen M. (2020). Purification of forest clear-cut runoff water using biochar: A meso-scale laboratory column experiment. *Water*, 12: 478, 2–14. <https://doi.org/10.3390/w12020478>
- III Kakaei Lafdani E, Lauren A, J Cvetkovic, Pumpanen J, Saarela T, Palviainen M. (2021). Nitrogen recovery from clear-cut forest runoff using biochar: adsorption–desorption dynamics affected by water nitrogen concentration. *Water, Air, & Soil Pollution*, 232:432, 1-15. <https://doi.org/10.1007/s11270-021-05366-y>

In article I: Elham Kakaei Lafdani took part in the writing and revision of the article and the analyses of the data. Taija Saarela was responsible for the laboratory work and the data-analysis. The experiment design was conceived by Marjo Palviainen and Annamari Laurén. Marjo Palviainen and Jukka Pumpanen acquired the funding for this project.

In article II: Elham Kakaei Lafdani was the first author and carried out the experimental work, data-analysis and drafted the manuscript. Marjo Palviainen and Annamari Laurén formulated the idea and conceptualised the study design. Marjo Palviainen, Annamari Laurén and Jukka Pumpanen acquired the funding. Taija Saarela carried out the sampling and experimental work, and also provided feedback on the manuscript. Jukka Pumpanen contributed to drafting the manuscript.

In article III: Elham Kakaei Lafdani, Marjo Palviainen and Annamari Laurén formulated the idea and conceptualised the study design. Elham Kakaei Lafdani was the first author, set up the experiment, carried out the experimental work and data-analysis, and drafted the manuscript. Jovana Cvetkovic contributed to water sampling. Taija Saarela carried out the experimental work and provided feedback on the manuscript. Jukka Pumpanen, Marjo Palviainen and Annamari Laurén contributed to drafting the manuscript. Marjo Palviainen and Jukka Pumpanen provided the funding for this project.

TABLE OF CONTENTS

ABSTRACT	3
ACKNOWLEDGEMENTS	4
LIST OF ORIGINAL ARTICLES	5
LIST OF ABBREVIATIONS	7
1 INTRODUCTION	9
1.1 Background	9
1.2 Peatland forest clear-cutting and water quality	10
1.3 Peatland forestry and water protection	11
1.4 Adsorption-based water protection method	12
1.5 Research gaps	13
1.6 Objectives of the thesis	13
2 MATERIALS AND METHODS	15
2.1 Study area and water sampling	15
2.2 Experimental design	16
2.3 Chemical analyses	22
2.4 Statistical analyses	22
3 RESULTS	25
3.1 Variations in pH and EC values	25
3.2 Adsorption of TN	26
3.3 Adsorption of inorganic nitrogen	31
3.4 Changes in TOC and P concentrations	33
3.5 Residence time and N compound changes inside the biochar reactor	33
3.6 Desorption experiment	34
4 DISCUSSION	37
4.1 Adsorption of organic and inorganic nitrogen by biochar	37
4.2 Adsorption kinetics	39
4.3 Desorption dynamics	40
4.4 Biochar as a Water Protection Tool	40
5 CONCLUSION	43
REFERENCES	45

LIST OF ABBREVIATIONS

AIC	Akaike Information Criterion
BIC	Bayesian Information Criterion
C	Carbon
CO ₂	Carbon dioxide
DON	Dissolved organic nitrogen
CH ₄	Methane
K _{ad}	Adsorption rate
N	Nitrogen
N ₂ O	Nitrous oxide
NO ₂ ⁻ -N	Nitrite nitrogen
NO ₃ ⁻ -N	Nitrate nitrogen
NH ₄ ⁺ -N	Nitrogen ammonium
P	Phosphorus
Q _{max}	Adsorption capacity
RMSE	Root Mean Square Error
R ²	Coefficient of determination
SS	Suspended sediment
TN	Total nitrogen
TOC	Total organic carbon
α	Birch biochar
β	Spruce biochar

1 INTRODUCTION

1.1 Background

The demand for forest biomass is expanding in tandem with the move towards a sustainable bio-based economy. Finland has around 20 different tree species, but the most important for forestry are Scots pine (*Pinus sylvestris* L.), Norway spruce (*Picea abies* (L.) H. Karst), and silver birch (*Betula pendula* Roth). In mineral soils, pure Scots pine stands develop in very dry environments, while Norway spruce grows in more fertile areas and silver birch grows mostly in mixed forests. Mixed species forests compose more than half of all forests in the country (Marttila et al. 2005).

In Finland, a considerable proportion of the harvested forest biomass is produced in drained peatland forests. Drainage is required as the naturally high-water table poses limitations on the growth of trees in these soils (Sikström and Hökkä 2016). Since the early twentieth century, the drainage of peatlands has been a common feature of forestry practice in the Baltic countries, Fennoscandia, the British Isles, and some parts of Russia (Nieminen 2004). Peatlands encompass approximately 30% of the land area in Finland (Ahtikoski and Hökkä, 2019) and a significant proportion, accounting for over half of the peatlands in the country, has been subjected to drainage through ditching for forestry purposes (Päivänen and Hännell, 2012). The main tree species in peatland forests are Norway spruce, Scots pine, and downy birch (*B. pubescens* Ehrh.). Norway spruce is dominant on fertile spruce fens, whereas Scots pine is the dominant species in less fertile bogs (Päivänen and Hännell, 2012). In Finland, natural peatlands are no longer exposed to ditch draining, and peatland forestry practices are now focused on previously drained sites and on maintaining tree growth in those sites (Ministry of the Environment, 2006).



Figure 1. Area of ditch network maintenance in Finland between 2004–2020 (blue line, ha yr⁻¹), and the number of clear-cuts on both mineral and peatland sites (green line, ha yr⁻¹). Note: While the statistics do not separate the clear-cuts on the mineral and peatland sites, approximately 20% of forests are on drained peatlands (Luke statistics database, 2022).

The predominant forest regeneration strategy employed in drained peatlands entails a sequential process that encompasses clear-cutting, maintenance of the ditch network, site preparation and tree planting (Paavilainen and Päivänen, 1995). In Finland, the area of ditch network maintenance has decreased from 78,000 ha to 17,000 ha between 2004 and 2020 (Figure 1) (Luke statistics database, 2022). The practice of clear-cutting and the subsequent maintenance of ditch networks have been identified as significant contributors to the export of sediment and nutrients into various water bodies, such as brooks, rivers and lakes (Joensuu, 2002; Nieminen, 2003, 2004; Nieminen et al., 2010).

Clear-cutting on drained peatlands represents a recognised environmental hotspot with regard to water quality. It is associated with a substantial amplification in nutrient export and sediment transport, surpassing equivalent clear-cutting operations in mineral soil forests by a considerable magnitude (Finér et al., 2010). With the maintenance of the drainage network, erosion within the ditches becomes more pronounced, leading to a notable increase in sediment loads (Stenberg, 2016). Furthermore, since nitrogen (N) and phosphorus (P) adhere to the eroded material, the maintenance of the ditch network increases N and P loading. The water table rises when the stand is clear-cut, leading to increased runoff and the magnitude of nutrient loading (Sikström and Hökkä, 2016). Multiple negative impacts on the receiving aquatic ecosystems are caused by increased sediment and nutrient loading (Bilotta and Brazier 2008).

The threat to water quality is a growing concern because the large peatland forest areas that were drained for the first time during the 1960s–1980s are now reaching regeneration age, thereby increasing the area subject to clear-cutting in the near future. This is anticipated to result in increasing sediment and nutrient loading in water bodies, which underscores the need for the development of novel water protection approaches in peatland forestry.

1.2 Peatland forest clear-cutting and water quality

The contribution of Finland to nutrient loading in the Baltic Sea is noteworthy, as it represents over 10% of the total input (Rankinen et al., 2019). A recent ecological assessment of surface waters in the country underscores the urgent need to reduce nutrient export from rivers to improve the ecological status of the Baltic Sea (Rankinen et al., 2019). On a national scale, the annual exports of N and P from forested areas to the sea are estimated to reach approximately 18,000 Mg and 1,100 Mg, respectively. (Nieminen et al., 2020).

Undisturbed stands of boreal forests are N restricted, and the N cycle is largely closed (Palviainen et al., 2004). Most of the mineralised N is taken up by the roots of trees and ground vegetation, with minimal losses due to leaching (Tamm, 1991; Palviainen et al., 2004). However, clear-cutting has a number of effects on the distribution and fluxes of nutrients in forest ecosystems (Likens and Bormann, 1999): The soil gets warmer and more moist, and canopy shade, interception and water adsorption are reduced, resulting in enhanced logging residues and organic matter decomposition, and mineralisation of nutrients and nitrification (Palviainen et al., 2004). Harvesting decreases stand water and nutrient uptake and enhances runoff (Kreutzweiser et al., 2008). Excessive nutrient addition in the soil occurs at the same time as the soil's capability to adsorb and retain nutrients decreases. Consequently, there is an increase in nutrient export to the receiving water bodies and this contributes to the deterioration of aquatic ecosystems, including water quality degradation, eutrophication and the growth of harmful algal blooms (Conley et al., 2009). The impact can continue for an extended period, with notable effects observed within the initial three years following the clear-cutting operation (Rosén et al., 1996; Palviainen et al., 2014).

Logging residues represent a substantial proportion of the entire nutrient pool that was initially bound in the developing stand: In mature Norway spruce stands, logging residues contribute to almost 80% of the total N and up to 90% of the total P bound in the harvested stand (Palviainen et al., 2004). The carbon (C) content of logging residues is also high, as plant material contains around 50% C by dry mass (Killham, 1994). Considerable quantities of C are emitted into the atmosphere as carbon dioxide (CO₂) during the decomposition of the logging residues (Mattson et al., 1987). Studies have shown that a high nutrient concentration, low C/N and C/P ratios, an adequate N/P ratio, and a low lignin content all enhance decomposition (Palviainen et al., 2004).

In contrast to fine residues (foliage, fine roots and twigs), coarse residues (stumps, coarse roots and branches) decompose gradually and contain a large proportion of resistant organic substrates and low concentrations of nutrients (Hyvönen et al., 2000). Therefore, fine residues constitute the most significant source of nutrients following clear-cutting, while the nutrients in coarse residues do not become available for many years or even decades after the clear-cut (Hyvönen et al., 2000).

Clear-cutting of drained peatlands may also lead to a rise in the formation and leaching of easily soluble organic compounds. Lundin (1999) demonstrated that the possibility of accelerated leaching of dissolved organic carbon (DOC) due to clear-cutting is significant. Many nutrients are released into the soil after clear-cutting and, consequently, the nutrient outflow increases. Furthermore, climate change will almost certainly exacerbate the situation by speeding up the decomposition of the peat soil and the release of nutrients into the environment (Nieminen et al., 2017).

1.3 Peatland forestry and water protection

In addition to imposing restrictions on environmentally harmful activities, there are several preventative strategies in forestry for diffuse load minimisation. Overland flow fields, constructed wetlands, sedimentation ponds, sedimentation pits and peak-flow control are the main methods to control the diffuse loads. Sedimentation ponds and overland flow areas may be employed with drainage and ditch network maintenance (Matero, 2004). The goal of the sedimentation ponds is to improve water quality by allowing suspended sediments and sediment-bound contaminants to settle within the pond. Overflow fields and constructed wetlands are typically employed before the runoff can reach the water bodies (e.g., Joensuu, 2002; Väänänen et al., 2008). Sedimentation-based and flow-control water protection methods can retain coarse-textured mineral soil particles from the runoff waters or prevent ditch erosion in the first place (Liljaniemi et al., 2003; Nieminen et al., 2005a; Eskelinen et al., 2015). However, these water protection methods are not particularly effective in retaining the soluble nutrients. In addition, the efficiency has been observed to be insufficient during peak/high flow periods (Liljaniemi et al., 2003), when the majority of the annual contaminant export takes place (Marttila and Kløve, 2009). Constructed wetlands and overland flow fields can also capture dissolved nutrients (Hynninen, 2011) through uptake by the vegetation and microbes, although the efficiency decreases outside the growing season when the nutrient uptake is suppressed due to low temperatures (Joensuu et al., 2002; Nieminen et al., 2005b). Pond construction is expensive, and the ponds must be cleaned frequently as, over the course of time, they may become filled with sediments. Furthermore, pond efficiency may be reduced when the walls of the pond collapse.

Despite being maintenance-free and inexpensive, there are some detrimental impacts regarding buffer zones, particularly as their construction by rewetting and restoring drained

peatland habitats potentially enhances nutrient outflow. In addition, buffer areas may increase nitrous oxide (N₂O) and methane emissions (CH₄) (Hynninen, 2011). It has been demonstrated that the riparian buffer zones that surround water bodies effectively retain soluble nutrients within the soil and plant systems (Vikman et al., 2010). The fundamental problem with biologically-based water protection measures is that they are temperature-dependent, which means they are ineffective outside of the growing season and increased nitrate (NO₃⁻-N concentrations are an excellent illustration of this (Mattsson, 2010).

In boreal catchments where the cold environment causes significant changes in seasonal runoff and evapotranspiration, strong seasonal and inter-annual fluctuations in loading and concentrations is a common feature (Liljaniemi et al., 2003). Almost 50% of total leaching in a year occurs following high discharge conditions and snowmelt in the spring. Furthermore, runoff peaks increase after harvesting and drainage of peatlands (Liljaniemi et al., 2003). The high flow and a rather low concentration of nutrients in the water are two characteristics of nutrient export from forested areas. As a result, an effective water protection system needs to retrieve nutrients from a low concentration and a substantial volume of water (Mattsson et al., 2015). In addition, a water protection system must be cost-effective and be able to properly retrieve nutrients when nutrient concentrations and discharge volume vary seasonally.

1.4 Adsorption-based water protection method

There are several approaches for water purification (Nieminen et al., 2005a; Jafari et al., 2017; Asfaram et al., 2017), which are generally based on adsorption processes and attempt to adsorb both organic and inorganic impurities (Moussout et al., 2018; Battas et al., 2019). In chemical and water engineering, adsorption has been considered a viable, practical and cost-effective strategy for the removal of contaminants from polluted media (Konneh et al., 2021; Singh et al., 2018). Adsorption mainly refers to the entrapment of substances from liquids or gases to the interface of two phases, primarily onto solids (Pillai, 2020). The adsorption method requires adsorbents with high adsorption capacity (Cai et al., 2019), such as activated C, clay minerals, zeolites, metal oxides, agricultural wastes, biomass and polymeric materials. Activated C is a commonly used adsorbent in water purification. The adsorption effectiveness of activated C is primarily attributed to its substantial specific surface area and developed porous structure. Similar to activated C, biochar is derived as a by-product of pyrolysis, a process that involves the thermal treatment of organic substances, such as wood, straw or industrial residues (e.g., paper sludge and biosolids) under controlled oxygen-deficient conditions (Lehmann and Joseph, 2015).

Biochar has emerged as a promising alternative to activated C in the field of environmental remediation and water treatment. This is primarily due to its cost-effectiveness, the widespread availability of raw materials and its remarkable sorption capacity (Kearns et al., 2014). Biochar production involves the utilisation of thermochemical processes, such as gasification, slow pyrolysis and rapid pyrolysis. The physicochemical properties of biochar derived from each of these processes can vary, and they are predominantly influenced by factors, such as the reaction duration and temperature, the composition of the initial feedstock material, as well as the activation techniques employed (Inyang and Dickenson, 2015). Biogas and bio-oil are produced during the pyrolysis process, and the C-rich solid residue is referred to as biochar.

Biochar exhibits numerous similarities to activated C in various aspects. Biochar is a stable material and is characterised by a high C content. Biochar is created through the

process of pyrolysis, which involves the thermal decomposition of biomass (e.g., wood, agricultural waste or organic matter) in a low-oxygen or oxygen-free environment, typically at temperatures below 700°C (Beesley et al., 2011). Biochar exhibits effectiveness in the adsorption of various compounds from water, attributed to its porous structure, substantial specific surface area and notable cation exchange capacity (Mohan et al. 2014). The elimination of organic and inorganic contaminants by biochar involves various key mechanisms that include electrostatic interaction, ion exchange, pore filling and precipitation (Ambaye et al., 2021). The remarkable adsorption capacity of biochar can be attributed to its expanded microporous and aromatic structure, as supported by various studies (Srinivasan and Sarmah, 2015; Yu et al., 2018; Liu et al., 2020). Moreover, biochar has shown greater adsorption capabilities than activated C in multiple investigations (e.g., Inyang and Dickenson, 2015; Dalahmeh, 2016). Yao et al. (2012) confirmed that increasing the pyrolysis temperature of biomass, for example to 600°C, enhances its adsorption capacity. Largette and Pasquier (2016) categorised the adsorption process into three stages: i) external mass transfer, where the adsorbate moves from the bulk solution to the external surface of the adsorbent, ii) internal diffusion, involving the movement of the adsorbate to the sorption sites, and iii) actual sorption. The first two processes are particularly affected by the biochar particle size. As a result, biochar may be a less expensive alternative to activated C (Gwenzi et al., 2016). Moreover, biochar offers a wide range of environmental management applications, in particular, soil conditioning, remediation and C sequestration (Oliveira et al., 2018; Palviainen et al., 2018).

1.5 Research gaps

Previous studies have indicated the adsorption capabilities of biochar for water contaminants (Dai et al., 2020; Chand et al., 2022). However, it is important to consider that the chemical composition of runoff water differs significantly between peatland forests and agricultural or urban areas (Mattsson et al., 2015). The performance of biochar in the recovery of pollutants from runoff water may be influenced by the presence of various dissolved chemicals. This is attributed to simultaneous competition among multiple compounds for adsorption sites during the adsorption process (Palviainen et al., 2018). Furthermore, as the nutrient concentration in water increases, the adsorption capacity of biochar also increases (Ahmadvand et al., 2018). This suggests that the adsorption capacity of biochar can be influenced by seasonal fluctuations in nutrient concentrations in the runoff water. To date, there has been a lack of research on the effects of decreasing concentrations on the potential desorption of N, where the release of nutrients previously adsorbed onto the surface of biochar takes place. A full understanding of the desorption process of recovered N is crucial when biochar is utilised for water protection purposes. Consequently, the findings of earlier studies conducted in agricultural and urban contexts are not directly transferable to peatland forest environments.

1.6 Objectives of the thesis

The primary objective of this research thesis was to investigate the efficacy of biochar as a means of adsorption-based nutrient recovery from runoff water that specifically originated from forested areas. The study was carried out in two small-scale and one meso-scale laboratory experiments with biochar produced from Norway spruce and Silver birch chips.

The water samples utilised in the experiments were obtained from a specific drainage ditch that collected runoff water from a clear-cut peatland forest located in eastern Finland. More specifically, the objectives were:

Objective 1:

To examine the adsorption characteristics of biochar for various N compounds in forest runoff waters, alongside their correlation with birch and spruce biochar properties in a small-scale experimental setup with a small volume of runoff water (Paper **I**).

Objective 2:

To investigate the adsorption characteristics of organic N compounds and inorganic N components from natural runoff water in a meso-scale experimental set-up that utilised 1000 litres of forest runoff water that circulated inside a biochar reactor filled with spruce biochar (Paper **II**).

Objective 3:

To explore the adsorption-desorption behaviour of spruce and birch biochar under fluctuating TN concentrations in forest runoff water (Paper **III**).

In Paper **I**, we constructed a biochar reactor for water purification, and studied the adsorption rate of the biochar and its capacity to adsorb the dominant chemicals in the runoff water. In Paper **II**, a biochar reactor was used to evaluate the recovery of different N compounds in the runoff water that passed through biochar filled-columns. In Paper **III**, the effect of N concentration on the adsorption and desorption dynamics of biochar in runoff water was examined.

2 MATERIALS AND METHODS

2.1 Study area and water sampling

Runoff waters for all three experiments was collected from a drainage ditch located in Heinävesi, Finland. This ditch originates from a fertile spruce fen that underwent clear-cutting in August 2018 (Figure 2). The study area experiences an average annual temperature of 3.6°C and annual precipitation of 638 mm. The area of the entire catchment was 31.72 ha, with a clear-cut area of 2.57 ha.

Harvest included 319 m³ of Norway spruce (124 m³ ha⁻¹) and 239 m³ of silver birch (93 m³ ha⁻¹). The depth of the peat layer was 0.5–0.7 m, and the subsoil was clay. The runoff water from the clear-cut site drains into the oligo-mesotrophic, clear-water Lake Kermajärvi, which is located within the Vuoksi primary catchment area. The export of nutrients from managed peatland forests may negatively impact the *good ecological status* of oligo-mesotrophic clear-water lakes.

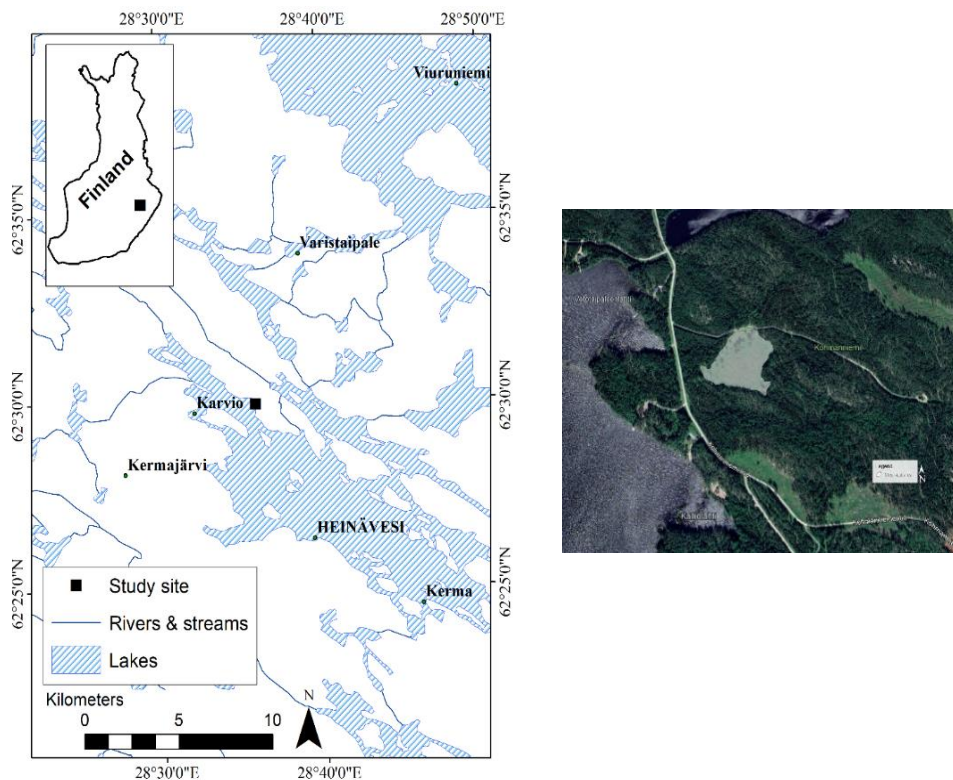


Figure 2. Location of the clear-cut area in Heinävesi, eastern Finland (PaTuli-spatial data for research and teaching; available at https://avaa.tdata.fi/en_US/web/paituli/latauspalvelu)

For the first experiment (Paper I), the water samples were collected in October and November 2018, from the main drainage ditch that collects runoff water from the harvested area. The initial N concentrations in the November runoff samples ($1.4 \pm 0.05 \text{ mg L}^{-1}$ TN, $0.6 \pm 0.09 \text{ mg L}^{-1}$ $\text{NO}_3\text{-N}$, and $0.1 \pm 0.02 \text{ mg L}^{-1}$ $\text{NH}_4^+\text{-N}$) were found to be higher than the N compounds concentrations observed in the October water samples ($0.9 \pm 0.03 \text{ mg L}^{-1}$ TN, $0.2 \pm 0.01 \text{ mg L}^{-1}$ $\text{NO}_3\text{-N}$, and $0.05 \pm 0.03 \text{ mg L}^{-1}$ $\text{NH}_4^+\text{-N}$).

In total, 1000 litres and 850 litres of runoff water were collected for the biochar reactor experiment (Paper II) on 21st January 2019 and 14th February 2019, respectively. On 22nd January 2019, the first phase of the experiment commenced with the injection of 1000 litres of collected runoff water (January water samples) into the water tank of the biochar reactor (capacity 3 m^3). After 3 weeks, the next phase of the experiment was initiated by adding 850 litres of water (February water samples) into the reactor system. The experiment continued for a duration of two months until March 22nd 2019.

For the adsorption-desorption experiment (Paper III), water sampling took place outside the growing season (November 2019) from the same ditch. The concentration of TN in the runoff water sample was 4.6 mg L^{-1} and prior to the experiments, the water was kept at a temperature of 4°C until the commencement of the experiment described in Paper III.

2.2 Experimental design

In this thesis, we used two commercial biochars manufactured by Carboflex Ltd., Tampere, Finland. These biochars were created from Silver birch and Norway spruce chips, employing a slow pyrolysis technique at a temperature of 600°C . Electric conductivity (EC) and the pH of the biochars were determined by preparing a 1:12.5 v:v solution of biochar and water. In addition, the N_2 adsorption technique was employed with a Micromeritics Flowsorb II 2300 instrument to determine the specific surface area of the biochar (Micromeritics Flowsorb II 2300, 1986). Detailed information on the properties of the two biochars are shown in Table 1.

In Experiment I, we selected two biochar doses (3 g and 12 g) and two grain sizes (fine and coarse). The size of the fine and coarse particles were approximately 4 mm and 4–6 mm, respectively. The primary objective was to assess the impact of grain size and dose on the adsorption characteristics of the biochars. A total of four replicates were considered for all treatments. The October and November water samples were utilised for replicates 1&2 and replicates 3&4, respectively.

To control the potential impact of temperature on the adsorption process, the runoff water temperature in all replicates was kept at a stable 21°C before initiation of the experiment. This step was taken as temperature had been identified to have the potential to influence the adsorption process (Mizuta et al., 2004). This corresponds to the upper range of air temperature expected under field conditions, where the air temperature ranges from -25°C to 25°C . For all treatments, biochar was placed into three 3000 mL glass jars, and the fourth jar was left as a blank sample. Then, 2500 mL of runoff water was poured into the jars, and 60 mL of water was removed to measure the initial nutrient concentrations in each jar. All jars were covered with aluminium foil.

Table 1. Characteristics of the Norway spruce (*Picea abies*) and Silver birch (*Betula pendula*) biochars. Mean and standard deviation (in parentheses) are shown.

Biochar properties	Norway spruce	Silver birch
Particle size (mm) (Experiment I)	4–6	4–6
	< 4	< 4
Particle size (mm) (Experiment II)	< 8	-
Particle size (mm) (Experiment III)	4–6	4–6
Pyrolysis temperature (°C)	600 °C	600°C
Electric conductivity ($\mu\text{S cm}^{-1}$) (1:2.5 v: v biochar/water solution)	221 (15)	163 (3)
pH (1:2.5 v: v biochar/water solution)	9.25 (0.01)	9.75 (0.02)
Specific surface area ($\text{m}^2 \text{g}^{-1}$)	320	260
N%	1.19 (0.09)	1.39 (0.15)
C%	79.07 (0.83)	80.00 (0.05)
C:N ratio	66.9 (5.51)	58.2 (6.38)
Dry matter (%) (105 °C, 48 h)	72.6 % (2.74)	81.0% (1.86)

The jars were placed on a shaker (New Brunswick™ Innova® 2300, Eppendorf Nordic A/S, Denmark) at a speed of 105 rpm for 10 days. Water samples (60 mL) were taken at 1, 2.33, 5.5, 25, 28, 46, 49, 70, 145, 169, 196, and 215 hours after the start of experiment (Paper I). All water samples were filtered by Filtration Assembly with Whatman GF/F Glass Microfiber Filters (pore size 0.7 μm , GE Healthcare Bio-Sciences, Marlborough, MA, USA).

In Experiment II, a biochar reactor (Figure 3) was used to retain organic N and inorganic N from the runoff water. The reactor consisted of three horizontal PVC plastic columns (inside diameter: 150 mm; length: 150 cm) with both sides of the columns were covered by PVC caps. All columns were filled to capacity without being compressed with spruce biochar having particle size < 8 mm. The column volume and dry bulk density of the biochar were 0.0265 m^3 and 200 kg m^{-3} , respectively. Therefore, the amount of biochar mass within each column equalled 5.3 kg. In this reactor, the tank of water was positioned at the height of 3 m above the columns and runoff was circulated through the three parallel columns. The cumulative effect of the purification can be monitored by recirculation of the water through the reactors. The fundamental properties of the collected water sample are illustrated in Table 2.

In the first stage of Experiment II, a total of 1000 L of runoff water were circulated through the biochar reactor for 21 days (total of 23 cycles). Then, in the second stage, an additional 850 L of runoff water was added into the system due to the complete adsorption of all mineral N, thereby prolonging the experiment for an additional 37 days. During the first week of the experiment, 50 mL water samples were collected three times daily. In the second week, the frequency of sampling was reduced to twice daily. Subsequently, for the remainder of the experiment, water samples were collected once daily. The filtration assembly employing Whatman GF/F Glass Microfiber Filters, which had a pore size of 0.45

μm , was utilised to filter all water samples (GE Healthcare Bio-Sciences, Marlborough, MA, USA). Following filtration, all water samples were stored at a temperature of 4°C until they were ready for subsequent analysis. The measurement of TN was conducted within one month after sampling, while the analysis of the mineral N fractions took place within one week.

Table 2. Initial characteristics of the collected water sample.

Parameter	Value	Parameter	Value
pH	7.24	Mg (mg L^{-1})	1.208
$[\text{H}^+]$	5.75×10^{-8}	Na (mg L^{-1})	1.984
EC	168	P (mg L^{-1})	0.026
TOC (mg L^{-1})	0.0319	Pb (mg L^{-1})	0.225
TN (mg L^{-1})	0.828	S (mg L^{-1})	3.271
$\text{NH}_4^+\text{-N}$ (mg L^{-1})	0.066	Si (mg L^{-1})	7.210
$\text{NO}_3^-\text{-N}$ (mg L^{-1})	0.251	Zn (mg L^{-1})	0.247
Al (mg L^{-1})	0.313	K (mg L^{-1})	3.668
Ca (mg L^{-1})	7.215	Fe (mg L^{-1})	0.406
Mn (mg L^{-1})	0.087	-	-



Figure 3. Experimental set-up of the biochar reactor.

The control of water inflow and outflow within the columns was facilitated through the utilisation of adjustable valves located on the caps. These valves allowed for precise regulation of the water flow in both directions. Water samples were extracted from the hoses that were connected to both the reactor outlets and inlets. In order to mimic the low water flow velocity in the ditches of forested peatlands (Haahti 2018), the rate of water flow (L min^{-1}) passing through the columns was measured using a graduated cylinder and a stopwatch. This approach provided a reliable means to track and record the rate at which the water passed through the system on a day-to-day basis. The valves were utilised to regulate the flow and to ensure that it stayed within the desired range when the recorded flow rate exceeded the specified $0.5\text{--}1 \text{ L min}^{-1}$ range. As such, the velocity of water inside the columns and the residence time were kept within $0.001\text{--}0.002 \text{ m s}^{-1}$ and $12\text{--}23 \text{ min}$, respectively.

Experiment **III** contained separate set-ups for the determination of TN adsorption under different TN concentrations in the water (Adsorption set-up, Figure 4); and to determine the TN desorption that potentially occurs when the TN concentration declines after preceding adsorption (Desorption set-up, Figure 5). In order to analyse the effect of N concentration on adsorption, the dilution of runoff water by milli-Q water was carried out to achieve targeted TN concentrations of $1, 2, 3,$ and 4 mg L^{-1} . Prior to the experiment, the collected runoff water was given sufficient time to stabilise at a temperature of 21°C . Then, 1 L of runoff water was treated with 5 g of spruce or birch biochar. Each individual concentration had three biochar replicates and one non-biochar control. At a consistent speed of 110 rpm , glass jars were shaken for a duration of 10 days . During this period, 30 ml water samples were extracted from each treatment at eight different time steps: $0, 2, 5, 25, 48, 72, 125,$ and 173 hours .

The experimental setup of Experiment **III** consisted of two distinct phases, namely an adsorption phase and a desorption phase (Figure 5). In the adsorption phase, birch and spruce biochar were exposed to four different TN concentrations and TN was allowed to sorb onto the biochar surfaces and structures. Thereafter, the biochar was extracted, and in the desorption phase, it was exposed to considerably lower concentrations to study the possible release of TN from the adsorbed storage.

The adsorption phase was initiated by blending 5 g of each type of biochar with 1 L of runoff water. To ensure accuracy, this process was replicated three times for each of the four distinct TN concentrations. The runoff water was carefully diluted with milli-Q water to achieve TN concentrations of $1, 2, 3,$ and 4 mg L^{-1} . The adsorption phase was monitored for a duration of 72 hours , thereby facilitating comprehensive analysis and assessment of the adsorption capability of both biochars. In the desorption phase, the biochars were filtered and separated into two 2.5 g (dry mass) samples. The biochar samples were then placed inside the glass containers, where they underwent stirring using the milli-Q water. The water was carefully diluted to achieve the lower concentrations of 0.2 mg L^{-1} and 0.35 mg L^{-1} , thereby providing the necessary concentration of TN for the desorption process. After 9 days of shaking at 110 rpm , water samples were extracted. Similar to the Experiment **II**, the filtration assembly was utilised to filter all water samples.

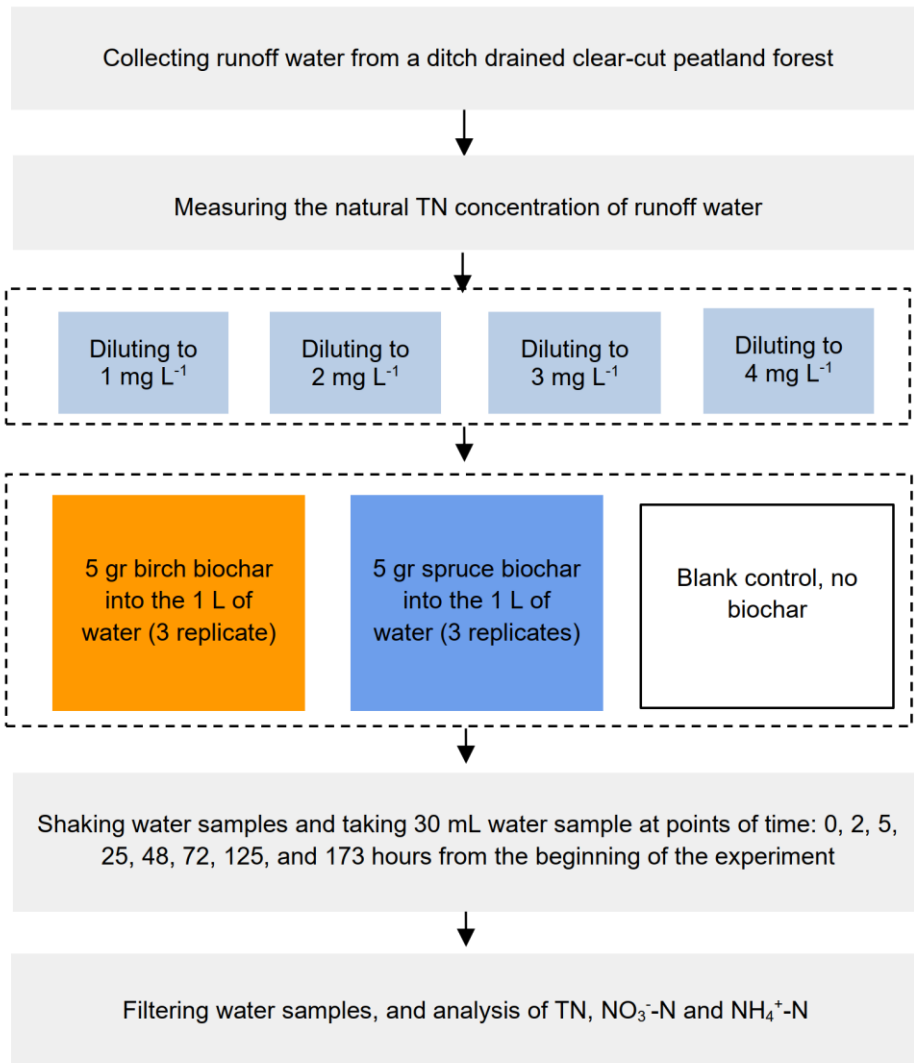


Figure 4. Experimental design of the adsorption setup.

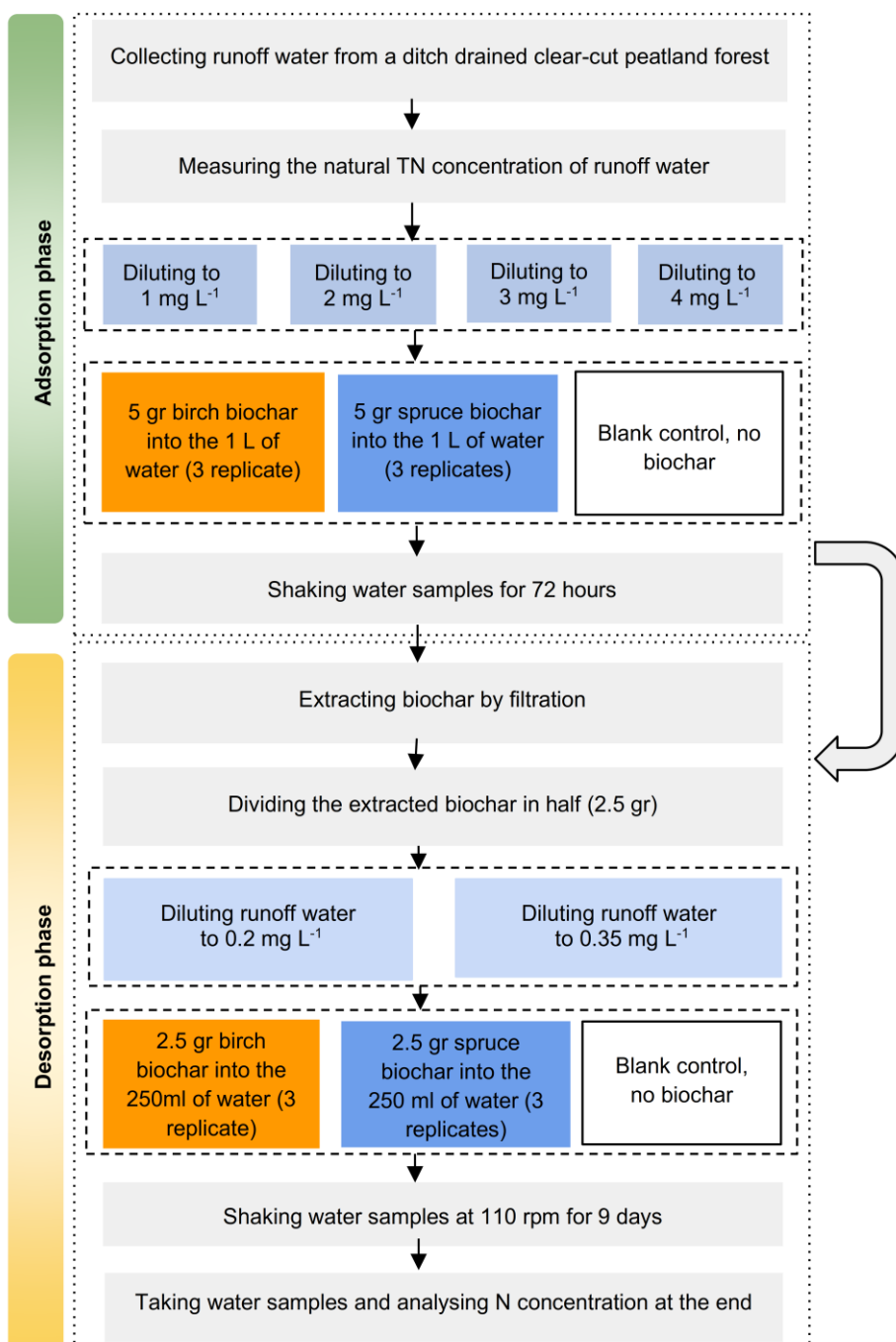


Figure 5. Experimental design of the desorption setup.

2.3 Chemical analyses

Electrical conductivity (EC) and the pH of the runoff water and biochar (in a 1:2.5 v:v biochar/water solution) were measured using a WTW pH/cond 340i and WTW pH 340i (WTW GmbH, Weilheim, Germany), respectively. In addition, the N₂ adsorption technique was employed to determine the specific surface area of the biochar with a Micromeritics Flowsorb II 2300 instrument. This approach involves the physical adsorption of a gas onto the surface of the biochar, which permits the quantification of the amount of adsorbate gas required to form a monomolecular layer on the surface. Moreover, the dry mass of the biochar sample was determined by placing it in an oven at 105°C for 48 hours.

The C and N contents in the biochars were determined using a Vario Max CN elemental analyser (Elementar Analysensysteme GmbH, Germany). The Multi N/C® 2100 instrument (Analytik Jena AG, Jena, Germany) was used to measure the concentrations of TN and total organic carbon (TOC). Quantification of NO₃⁻-N and ammonium (NH₄⁺-N) was carried out using the colorimetric evaluation methods developed by Fawcett and Scott (1960) and Miranda et al., (2001).

To ensure accurate measurements, a detection limit of 0.02 mg L⁻¹ was established for NO₃⁻-N and NH₄⁺-N. This threshold signifies the minimum concentration that could be reliably detected by the analytical method employed. In cases where the measured values fell below this limit, a data adjustment was applied, which reduced the values to 50% of the established threshold (Sigh and Nocerino, 2002). Concentrations of P were analysed with an ARL 3580 OES ICP atomic emission spectrophotometer (Fison Instruments, Valencia, USA).

2.4 Statistical analyses

The adsorption of N compounds and TOC ($A_{t,p}$) to the birch and spruce biochars was calculated using the concentration changes of the substance in the water samples (Equation 1):

$$A_{t,p} = \frac{(c_{ini,p}v_{ini}) - \sum_{t=ini}^n (c_{t-1,p} - c_{t,p})v_{t-1,t}}{m_{biochar}} \quad (1)$$

Variable A_{tp} (mg g⁻¹ biochar) represents the cumulative adsorption amount of substance p , where p can refer to TN, NO₃⁻-N or NH₄⁺-N. The initial concentration of component p and the initial volume of water are shown as $c_{ini,p}$ (mg L⁻¹) and v_{ini} (L), respectively. The component concentration of p at time t is indicated as $c_{t,p}$ (mg L⁻¹), while the component concentration at time t^{-1} is denoted as $c_{t-1,p}$ (mg L⁻¹). The volume of water from time t^{-1} to t is denoted as $v_{t-1,t}$ (L). In addition, the dry mass of biochar is represented by $m_{biochar}$.

Linear mixed-effect models were employed in Experiment I and in the adsorption set-up of Experiment III to explore the relationship between the initial concentration and the cumulative adsorption of TN at the end of each experiment. Within the model framework, biochar type and concentration were treated as fixed effects. In addition, the replicates were considered as random effects.

$$A_{t, end, pi} = \alpha_{p,i} + \beta_{p,i} C_{ini,p,i} + \varepsilon_{p,ij} \quad (2)$$

The cumulative desorption amount of TN and NO_3^- -N compounds (p) from biochar i at the end of the experiment is denoted as $A_{t \text{ end},p}$ (mg g^{-1} biochar). In this equation, the adsorption process is influenced by fixed parameters, $\alpha_{p,i}$ and $\beta_{p,i}$, which are specific to biochar i and the p component. The initial concentration of the p component is denoted as $C_{\text{ini},p}$ and is measured in mg L^{-1} . The term ε_{pij} represents the residual term for the p component and biochar i, along with the replicant j. The mean expected value for ε_{pij} is equal to 0.

To evaluate the performance of the model, several criteria were employed, including Akaike Information Criterion (AIC), Bayesian Information Criterion (BIC), log likelihood, Root Mean Square Error (RMSE), and coefficient of determination (R^2). These criteria provide a quantitative assessment of how well the model fits the data and captures the underlying patterns. Quantification of the desorption amount during the desorption phase of Experiment **III** was carried out using the following calculation:

$$D_{ci} = \frac{(c_{\text{end}} - c_{\text{ini}})v}{m_{\text{biochar}}} \quad (3)$$

Where D_{ci} represents the desorption amount of TN for biochar i (Bb, Sb) at a concentration of c, which can take the values of 0.20 or 0.35 (mg L^{-1}). c_{end} (mg L^{-1}) and c_{ini} (mg L^{-1}) refer to the TN concentration in the solution at the end and beginning of the desorption phase, respectively. v (L) denotes the volume of the solution and m biochar represents the mass of the biochar.

To investigate the impact of the initial TN concentration on the desorption of TN during the desorption phase described in Experiment **III**, the cumulative desorption amount of TN at the end of the experiment (D_{216h}) was examined. Linear mixed-effect models (Equation 4) were employed for this analysis. In the model, biochar type and initial concentration were treated as fixed effects, while replicates were considered random effects:

$$D_{216,i} = \alpha + \alpha_S + (\beta + \beta_S) X_{\text{ini},i} + \varepsilon_{ij} \quad (4)$$

In equation (4), $D_{216,i}$ (mg g^{-1} biochar) represents the TN desorption of biochar i at a specific time (216 h). Parameters α and β are fixed constants specific to birch biochar, while α_S and β_S represent fixed parameters of spruce biochar and represent the differences from the fixed parameters of the birch biochar. The initial concentration of TN is denoted as X_{ini} , and its value can be either 0.2 or 0.35 mg L^{-1} depending on the particular conditions of the experiment. Furthermore, equation (4) incorporates the term ε_{ij} , which represents the residual term for TN in biochar i and replicate j. The expected value of ε_{ij} is 0. The adsorption kinetics were determined using integral forms of pseudo-first order (Equation 5) and pseudo-second order (Equation 6) adsorption models, as proposed by Largitte and Pasquier (2016).

$$A_p = Q_{\text{max},p} (1 - e^{-k_{\text{ad}1,p} t}) \quad (5)$$

$$A_p = \left(\frac{k_{\text{ad}2,p}^2 Q_{\text{max}1,p} t}{1 + k_{\text{ad}2,p} Q_{\text{max}1,p} t} \right) \quad (6)$$

In the given equation, A_p (mg g^{-1} biochar) represents the cumulative adsorption of NO_3^- -N and TN onto the biochar material at a specific time t (h). $k_{\text{ad}1,p}$ (h^{-1}) and $k_{\text{ad}2,p}$ ($\text{mg g}^{-1} \text{h}^{-1}$) refers to the adsorption rate of p components in the pseudo-first order and pseudo-second

order models, respectively. Both $Q_{\max,p}$ and $Q_{\max1,p}$ (mg g^{-1} biochar) refer to the maximum adsorption capacity of component p at equilibrium.

In the Paper I, noticeable differences in both Q_{\max} and k_{ad} were observed between the October 2018 and November 2018 water samples. These findings strongly suggest that the concentration of the components directly influences the magnitude of adsorption.

3 RESULTS

3.1 Variations in pH and EC values

In Experiment I, both biochars increased water pH by between 0.4 to 0.6 units when the dose was 3 g, and by between 0.6 to 0.9 pH units when the dose was 12 g (Figure 6). Electrical conductivity (EC) increased by 20% at both biochar doses (Figure 7) and with both biochars.

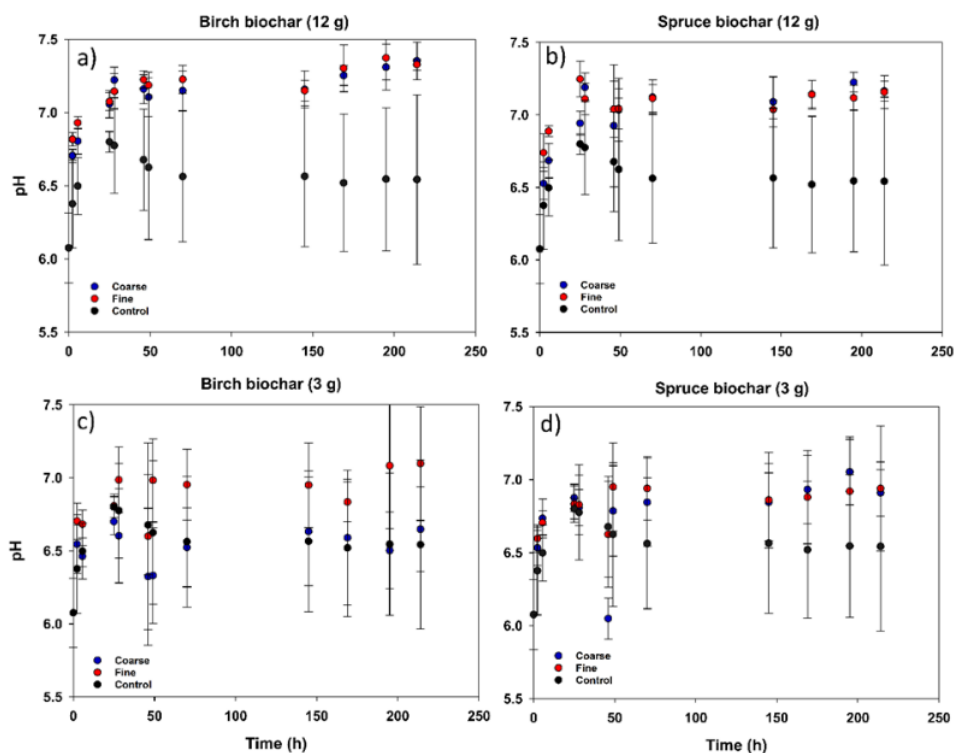


Figure 6. Impact of different biochar doses on pH levels (Experiment I). The reported values are presented as mean \pm standard deviation. Coarse particle size is represented by blue dots, fine particle size by red dots, and blank samples by black dots.

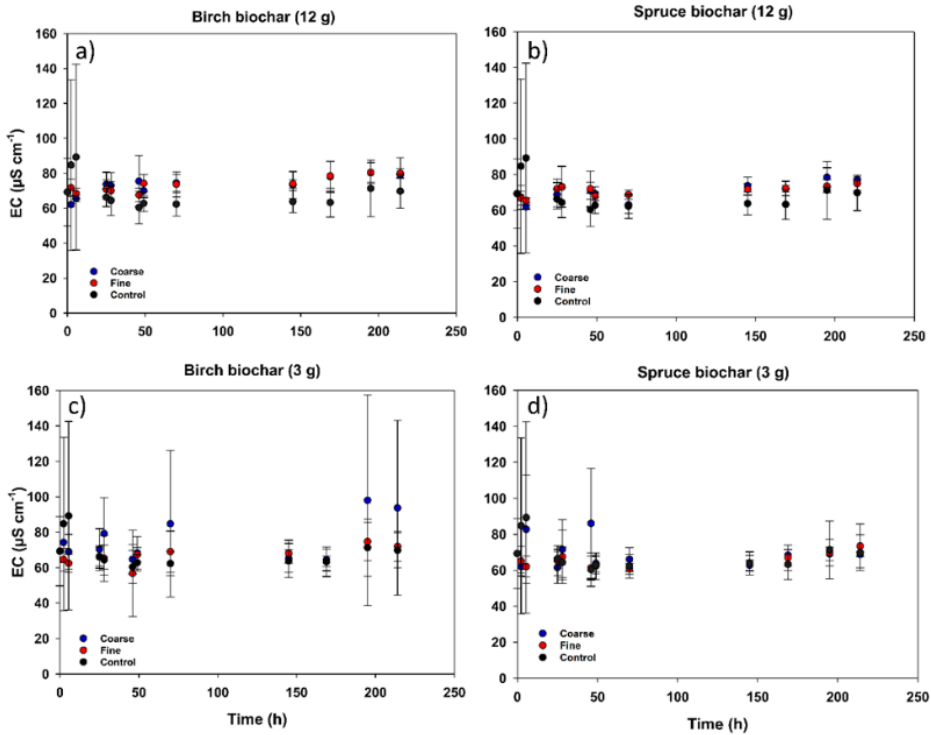


Figure 7. Impact of different biochar doses on electrical conductivity ($\mu\text{S cm}^{-1}$, Experiment I). The reported values are presented as mean \pm standard deviation. Coarse particle size is represented by blue dots, fine particle size by red dots, and blank samples by black dots.

3.2 Adsorption of TN

The results showed that the TN concentrations were decreased in all three experiments (**I**, **II** and **III**) using different biochar treatments (Table 3). In Experiment **I**, the greatest reduction in TN concentration was observed in the first 70 hours of the experiment. In the biochar reactor (Paper **II**), the TN concentration declined from 0.8 mg L^{-1} to 0.56 mg L^{-1} within the first three days, and gradually decreased subsequently. After 21 days, the TN concentration increased when 850 L of fresh runoff was fed into the reactor tank.

A 56% purification effectiveness was achieved in the first phase of experiment described in Paper **II**, when the TN concentration was reduced from an initial level of 0.8 mg L^{-1} to 0.35 mg L^{-1} . In Experiment **III**, the TN concentration rapidly decreased after 50 hours from the start of the experiment. The reduction in TN concentration in Experiments **I**, **II** and **III** revealed TN adsorption by the birch and spruce biochars. The TN adsorption rate and TN maximum adsorption capacity were determined using repeated water sampling and the measured gradual decrease of TN in the water (Table 4). For all three experiments, adsorption was rapid over the first few days but thereafter slowed down (Figure 8).

Table 3. Changes in TN concentration in the experiments.

Experiment	Biochar	weight (g)	size (mm)	Water volume (L)	Initial TN concentration (mg L ⁻¹)	Final TN concentration (mg L ⁻¹)
Experiment I	Birch	12	< 4	2	0.9	0.77
					1.4	1.1
		12	4 - 6	2	0.9	0.8
					1.4	1.04
	Spruce	12	< 4	2	0.9	0.88
					1.4	1.14
		12	4 - 6	2	0.9	0.88
					1.4	1.27
	Birch	3	< 4	2	0.9	0.84
					1.4	1.26
		3	4 - 6	2	0.9	0.875
					1.4	1.365
Spruce	3	< 4	2	0.9	0.91	
				1.4	1.33	
	3	4 - 6	2	0.9	0.885	
				1.4	1.52	
Experiment II	Spruce	5300*	< 8	1000	0.8	0.35
				850	0.81	0.41
Experiment III	Birch	5	4 - 6	1	1.0	0.45
					2.0	0.99
					3.0	1.60
					4.0	2.14
	Spruce	5	4 - 6	1	1.0	0.52
					2.0	1.13
					3.0	1.77
					4.0	2.45

*Mass of biochar inside each column

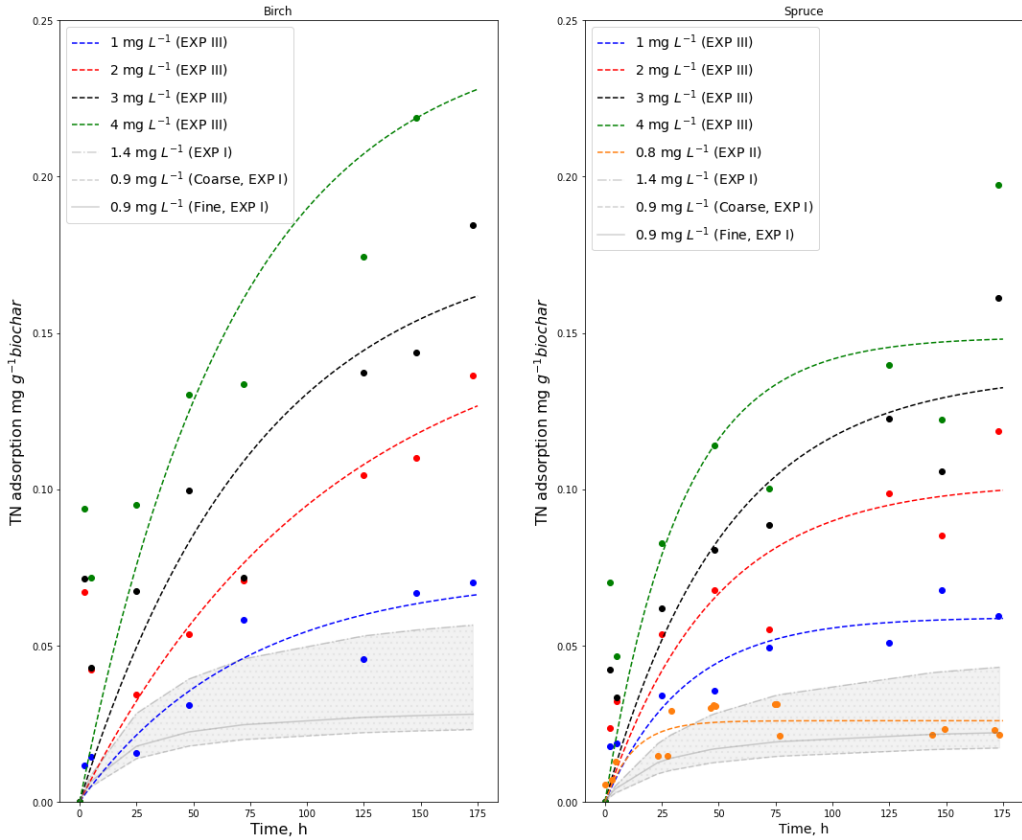


Figure 8. Biochar TN adsorption under a range of initial TN concentrations. Dashed lines represent a pseudo-first order kinetic model for Experiments II and III, while the grey lines represent a pseudo-second order kinetic model for Experiment I. The grey area demonstrates the range of adsorption variability observed between the coarse and fine biochar sizes and the initial TN concentrations of 1.4 mg L⁻¹ and 0.9 mg L⁻¹.

In Experiment III, TN adsorption was monitored in all biochar treatments, and the amount of adsorption varied depending on the initial TN concentration (Equation 2, Figure 9). For the spruce biochar, adsorption increased linearly from 0.05 to 0.2 mg TN g⁻¹ biochar, and for the birch biochar, from 0.07 to 0.3 mg TN g⁻¹ biochar. It is noteworthy that the birch biochar demonstrated a greater TN adsorption capacity than the spruce biochar (Figure 9). The results in Experiment II revealed that TN adsorption was not observed when the water TN concentration inside the reactor columns fell below 0.4 mg L⁻¹ (Figure 9). These findings demonstrate that the adsorption capacity of biochar is highly influenced by the N concentrations in the water (Figure 9). In particular, the adsorption capacity of the biochar showed a corresponding increase when the TN concentration in the water increased.

Table 4. TN adsorption parameters of the kinetic models.

Experiment	Biochar	weight (g)	size (mm)	Initial TN concentration (mg L ⁻¹)	Model			
					Pseudo-first order		Pseudo-second order	
					k _{ad1} (h ⁻¹)	Q _{max1} (mg g ⁻¹)	k _{ad2} (mg h ⁻¹)	Q _{max2} (mg g ⁻¹)
Experiment I	Birch	12	< 4	0.9	-	-	1.721	0.031
				1.4	-	-	0.417	0.068
			4 - 6	0.9	-	-	1.721	0.026
				1.4	-	-	0.417	0.068
	Spruce	12	< 4	0.9	-	-	1.721	0.025
				1.4	-	-	0.417	0.054
			4 - 6	0.9	-	-	1.721	0.02
				1.4	-	-	0.417	0.054
	Birch	3	< 4	0.9	-	-	0.222	0.084
				1.4	-	-	0.154	0.144
			4 - 6	0.9	-	-	0.222	0.065
				1.4	-	-	0.154	0.07
Spruce	3	< 4	0.9	-	-	0.222	0.085	
			1.4	-	-	0.154	0.089	
		4 - 6	0.9	-	-	0.222	0.055	
			1.4	-	-	0.154	0.015	
Experiment II	Spruce	5300*	< 8	0.8	0.150	0.020	19.830	0.020
Experiment III	Birch	5	4 - 6	1	0.017	0.059	0.190	0.079
				2	0.015	0.120	0.130	0.140
				3	0.022	0.140	1.050	0.120
				4	0.024	0.190	0.820	0.170
	Spruce	5	4 - 6	1	0.038	0.051	1.490	0.054
				2	0.033	0.084	0.750	0.089
				3	0.027	0.110	0.350	0.120
				4	0.170	0.120	1.400	0.130

*Mass of biochar inside each column

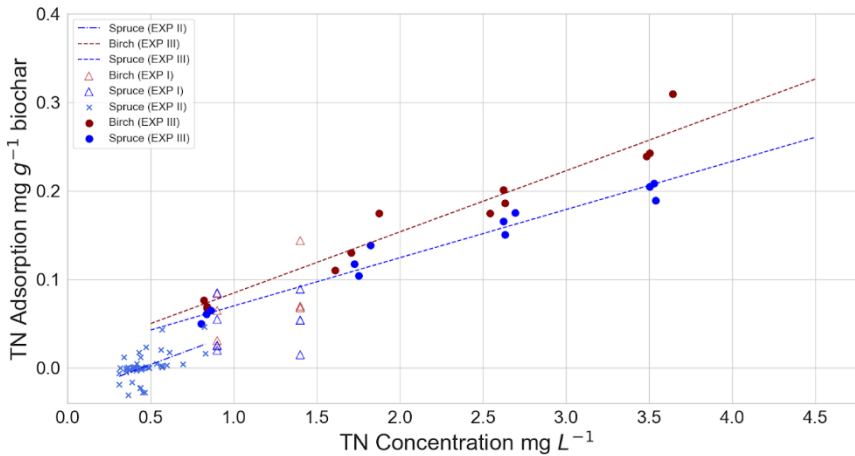


Figure 9. TN adsorption in the range of initial TN concentration changes in Experiments I, II and III. Blue and red correspond to spruce and birch biochars, respectively.

The pseudo-first order and pseudo-second order kinetic models were fitted to the adsorption results of Experiments II and III, while only the pseudo-second order model was provided for the results in Experiment I (Figure 8). For the adsorption capacity parameter, Q_{max} , the variations between the treatments were most noticeable in Experiment I (Table 4). Neither the initial concentration nor biochar type influenced the adsorption rate k_{ad1} (Experiment III, Table 4). The experimental results indicated that with an increase in the initial concentration of TN, there was a corresponding and consistent increase in Q_{max} (Experiments I, II and III; Table 4). At initial concentrations of 4 mg L^{-1} , Q_{max} was found to be approximately three to four times higher than Q_{max} values observed at an initial concentration of 1 mg L^{-1} (Experiment III, Table 4). The Q_{max} value of the birch biochar was greater than that of the spruce biochar (Table 4). Also, in most cases in Paper I, Q_{max} was almost two times greater at the initial concentration of 1.4 mg L^{-1} than at 0.9 mg L^{-1} . At higher concentrations, the adsorption process was more consistent (Experiment I, Figure 6). Furthermore, it was observed that birch biochar exhibited a higher Q_{max} value compared to the spruce biochar (Experiment I and III, Table 4). Higher biochar doses and TN concentrations (Experiment I, Table 4) resulted in a more consistent adsorption process (Figure 8). Particle size had no influence on k_{ad} , but smaller particle size resulted in increased Q_{max} (Experiment I, Table 4).

In the biochar reactor (Experiment II), the N adsorption kinetics were calculated based on the concentration change between the column inlet and outlet in the first phase of the experiment (Figure 8). The results of the pseudo-first and second-order models showed that Q_{max} for TN was $0.02 \text{ mg g}^{-1} \text{ biochar}$. In addition, k_{ad1} in the pseudo-first order model and k_{ad2} in the second-order model were 0.15 h^{-1} and $19.83 \text{ mg g}^{-1} \text{ h}^{-1}$, respectively (Experiment II). In the Experiment I (Figure 10a (weeks 2–3)), the adsorption model failed to capture the slow reduction in the N concentration. In the initial phase, the TN concentration decreased from 0.8 mg L^{-1} to 0.35 mg L^{-1} , and in the second phase, decreased from 0.81 mg L^{-1} to 0.41 mg L^{-1} , indicating adsorption of 1190 mg TN . The biochar reactor contained 15.9 kg of

biochar, resulting in TN adsorption of 0.07 mg g^{-1} biochar. As such, this amount of TN adsorption on biochar is about 3.5 times the value indicated by the estimated Q_{max} value.

3.3 Adsorption of inorganic nitrogen

In Experiments **I**, **II** and **III**, a decline in NO_3^- -N concentrations was observed in all samples treated with biochar, which indicates NO_3^- -N adsorption (Table 5). In Experiment **III**, the most substantial decrease in NO_3^- -N concentration was observed for the birch biochar samples at the higher TN concentration of 4 mg L^{-1} (Table 5).

Table 5. NO_3^- -N concentration changes

Experiment	Biochar	weight (g)	size (mm)	Water volume (L)	Initial NO_3^- -N concentration (mg L^{-1})	Final NO_3^- -N concentration (mg L^{-1})
Experiment I	Birch	12	< 4	2	0.185	0.045
			4 - 6	2	0.745	0.195
			< 4	2	0.205	-
			4 - 6	2	0.595	0.225
	Spruce	12	< 4	2	0.19	0.07
			4 - 6	2	0.57	0.325
			< 4	2	0.185	0.035
			4 - 6	2	0.695	0.35
	Birch	3	< 4	2	0.21	0.065
			4 - 6	2	0.475	0.37
			< 4	2	0.21	0.08
			4 - 6	2	0.55	0.48
Spruce	3	< 4	2	0.195	0.115	
		4 - 6	2	0.61	0.445	
		< 4	2	0.195	0.115	
		4 - 6	2	0.61	0.515	
Experiment II	Spruce	5300*	< 8	1000	0.18	-
			< 8	850	0.07	-
Experiment III	Birch	5	4 - 6	1	0.3	0.041
					0.67	0.59
					0.98	0.54
	Spruce	5	4 - 6	1	1.31	0.64
					0.3	0.02
					0.67	0.22
					0.98	0.92
					1.31	1.06

*Mass of biochar inside each column

Also, in Experiment **I**, the samples that contained 12 g of birch biochar showed a greater reduction in NO_3^- -N (Table 5) than treatments with the lower biochar dose. In addition, the initial concentrations of NO_3^- -N and NH_4^+ -N in the biochar reactor (Experiment **II**) were 0.18 mg L^{-1} and 0.066 mg L^{-1} , respectively.

At the start of the experiment, a significant reduction in NO_3^- -N and NH_4^+ -N concentrations were detected, and these declined below the detection limit within 5 days (Figure 10 c, d). In Experiment **I**, the reduction in NH_4^+ was more pronounced in samples with the 12 g biochar dose (Table 5). Throughout Experiment **III**, NH_4^+ -N concentrations consistently remained below the detectable threshold of 0.02 mg L^{-1} , thereby preventing the examination of concentration variations and adsorption characteristics (Table 5). When the adsorbing chemical in the water was reduced, the fitting of the adsorption model was incorrect, since Q_{max} no longer reflected the true adsorption capacity of the biochar. In Experiment **III**, when the initial concentration of NO_3^- -N increased from 0.2 to 1.4 mg L^{-1} , the adsorption of NO_3^- -N increased consistently, and as a result, the adsorption amount reached $0.15 \text{ mg NO}_3^- \text{ N g}^{-1} \text{ biochar}$ (Figure 9 and Table 5).

Nonetheless, the initial concentration of spruce biochar did not influence the adsorption of NO_3^- -N (Figure 9, Table 5). In Experiment **I**, the birch biochar treated samples exhibited the highest Q_{max} value for NO_3^- -N. Furthermore, Q_{max} typically showed an increasing trend at higher initial concentrations (Table 5). The size of the biochar particles had no noticeable influence on NO_3^- -N adsorption (Table 5). The NH_4^+ -N concentrations in all biochar treated samples were consistently low and rapidly decreased to levels below the threshold of 0.02 mg L^{-1} .

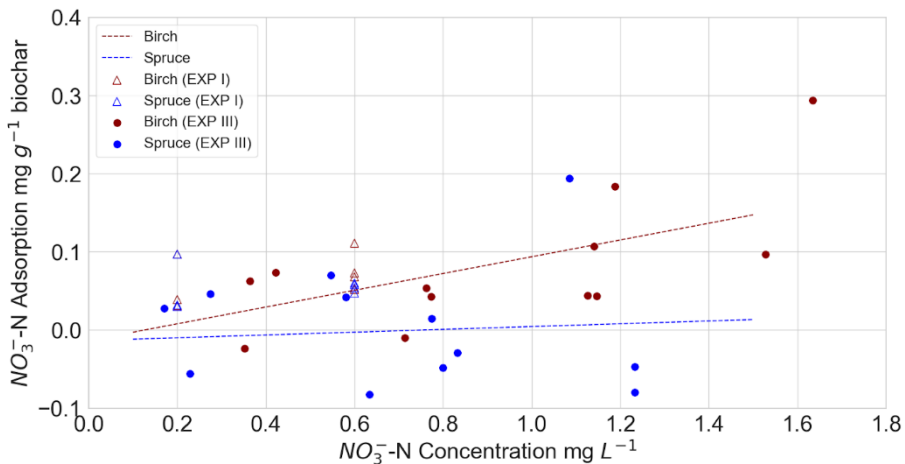


Figure 9. NO_3^- -N concentration and adsorption changes in all treatments in Experiments **I** and **III**.

3.4 Changes in TOC and P concentrations

In Experiment I, TOC concentrations in the water samples that had high initial values (28 mg L^{-1}) declined during the first two days of the experiment. After 145 hours, there were no significant differences in TOC concentrations between the biochar and control treatments. Furthermore, all treatments demonstrated an increase in TOC levels, which would indicate that TOC concentrations increased, irrespective of the specific treatment applied. During the entire experiment, P concentrations remained consistently below the detectable limit of 0.025 mg L^{-1} . Hence the adsorption parameters for P could not be determined.

3.5 Residence time and N compound changes inside the biochar reactor

In the biochar reactor (Experiment II), DON concentrations (obtained as the difference between TN and inorganic N) reduced from an initial concentration of $0.5\text{--}0.6 \text{ mg L}^{-1}$ to $0.3\text{--}0.4 \text{ mg L}^{-1}$ immediately following the addition of water (Figure 10b).

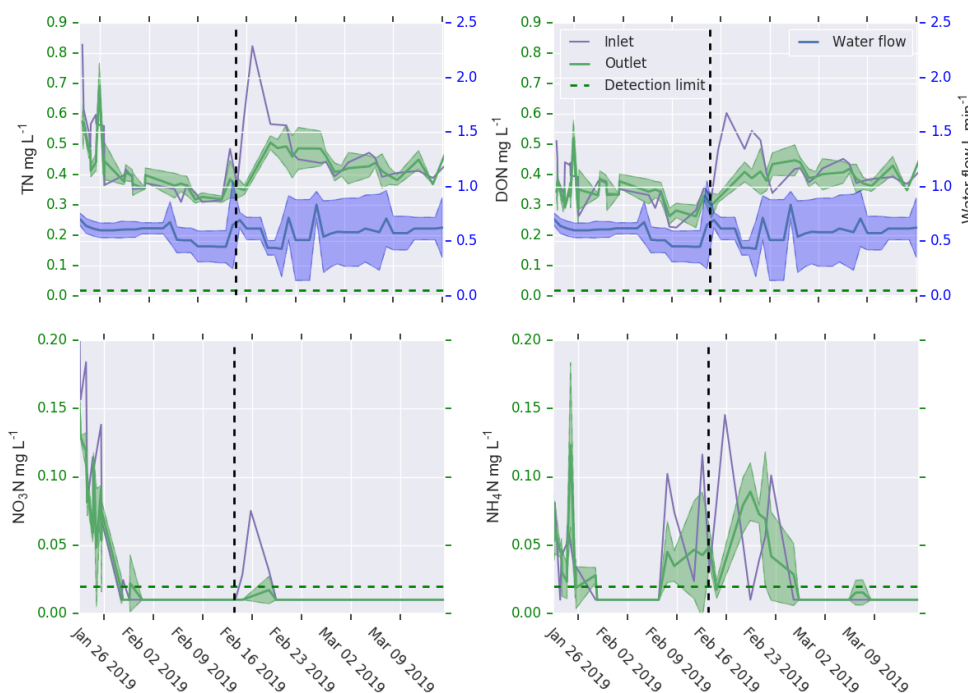


Figure 10. Variations in nitrogen (N) compounds in the column. Purple line and green line indicate N variation in the inlet and outlet of the column, respectively. The green area represents the mean outlet concentration \pm standard deviation. The blue line and area represent the mean water flow through the columns \pm standard deviation. The vertical dashed black line and the horizontal dashed green line indicate the time of water injection into the reactor tank and the detection limit, respectively.

The average water flow rate within the reactor columns varied between 0.45 and 0.8 L min⁻¹. The manipulation of the flow rate prior to and immediately after the introduction of water into the reactor had a direct influence on the concentrations of TN, DON and NH₄⁺-N, which would indicate that the duration of residence could potentially modify the adsorption process. The largest difference in concentrations between the inlet and outlet (indicating net adsorption) was observed when the TN concentration in the inflow exceeded 0.8 mg L⁻¹ (Figure 10). This finding suggests that the adsorption process was clearly influenced by the N concentration. Despite the absence of significant adsorption, evident from the distinction between the inlet and outlet, the temporal analysis of the inlet water concentration exhibited a gradual rate of water purification. Furthermore, the absorption of N subsequent to the injection of runoff water during the second phase of the experiment indicated that the biochar had not yet reached its saturation point.

3.6 Desorption experiment

During the adsorption phase of Experiment III, the birch and spruce biochars were both exposed to varying initial TN concentrations (1, 2, 3 and 4 mg L⁻¹). Subsequently, in the desorption phase, the extracted biochars were exposed to lower TN concentrations of 0.2 mg L⁻¹ and 0.35 mg L⁻¹ to investigate the occurrence of potential desorption (Table 6). The initial TN concentration had a noticeable impact on the desorption behaviour, especially for the birch biochar (Table 6).

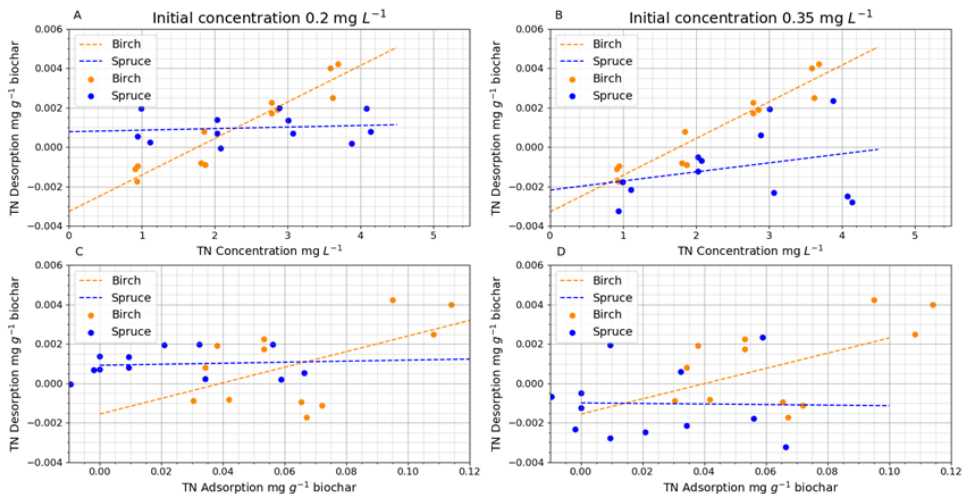


Figure 11. Desorption of TN from the biochar. Panels A and B show the desorption in correlation with TN concentration in the adsorption phase of the experiment, and panels C and D show the desorption in correlation with TN adsorbed onto the biochar. Negative desorption values imply that the biochar continues to adsorb TN at lower TN concentrations. The dashed lines show the linear mixed-effect models for the desorption (see parameters in Table 5).

Table 5. Linear mixed-effect models utilised to analyse TN desorption during the desorption phase of Experiment III. Panels A and B display the desorption trends in relation to the TN concentration during the adsorption phase, while panels C and D demonstrate the desorption patterns in relation to the TN adsorbed onto the biochar. Parameters α and β represent birch biochar, while the parameters for the spruce biochar are denoted as $(\alpha + \alpha_S)$ and $(\beta + \beta_S)$, respectively.

A	Value	StdError	DF	p-value	B	Value	StdError	DF	p-value
α	-0.003	<0.001	18	<0.001	α	-0.003	<0.001	18	0.003
α_S	0.004	<0.001	18	<0.001	α_S	0.001	<0.001	18	0.370
β	0.001	<0.001	18	<0.001	β	0.002	<0.001	18	<0.001
β_S	-0.001	<0.001	18	<0.001	β_S	-0.001	<0.001	18	0.007
RMSE	0.001	-	-	-	RMSE	0.001	-	-	-
AIC	-209.967	-	-	-	AIC	-187.107	-	-	-
log-Likelihood	110.983	-	-	-	log-Likelihood	99.553	-	-	-
F-value	39.88	-	-	-	F-value	22.739	-	-	-
Residual	0.001	-	-	-	Residual	0.001	-	-	-
C	Value	StdError	DF	p-value	D	Value	StdError	DF	p-value
α	-0.001	0.001	18	0.150	α	-0.002	0.001	18	0.290
α_S	0.002	0.001	18	0.040	α_S	0.001	0.001	18	0.740
β	0.40	0.014	18	0.020	β	0.039	0.019	18	0.060
β_S	-0.037	0.021	18	0.110	β_S	-0.04	0.028	18	0.170
RMSE	0.001	-	-	-	RMSE	0.001	-	-	-
AIC	-198.781	-	-	-	AIC	-187.278	-	-	-
log-Likelihood	105.390	-	-	-	log-Likelihood	99.643	-	-	-
F-value	0.004	-	-	-	F-value	0.002	-	-	-
Residual	0.001	-	-	-	Residual	0.001	-	-	-

Bold values are statistically significant.

Notably, the desorption patterns showed considerable variations between the spruce and birch biochars. At a TN concentration of 0.35 mg L^{-1} , spruce biochar displayed ongoing TN adsorption, as indicated by the negative desorption values (Figure 11B). When the initial TN concentration exceeded 1.8 mg L^{-1} during the adsorption phase, the desorption of TN from the birch biochar was noticeably greater than that from the spruce biochar (Figure 11A, B). The TN desorption of the birch biochar exhibited a relationship with the observed TN adsorption (Figure 11C, D). Birch biochar demonstrated TN release when the adsorption amount was $> 0.04 \text{ mg g}^{-1}$ biochar (Figure 11C, 11D). The TN was not markedly released from the spruce biochar in the water at 0.2 or 0.35 mg L^{-1} concentrations (Table 6C, 6D, Figure. 11). The amount of TN desorption by the spruce biochar in 0.2 mg L^{-1} was very low (Figure. 11A, 11C). Birch biochar desorption was more consistent at both concentrations (0.2

and 0.35 mg L^{-1}) (Figure 11). The desorption phase results indicate that the desorption process was concentration-dependent, and the magnitude of the desorption was very low being at maximum of only 2–4% of total adsorption.

4 DISCUSSION

4.1 Adsorption of organic and inorganic nitrogen by biochar

This thesis demonstrated that birch and spruce biochar efficiently adsorbed both organic and inorganic N from the water draining from a clear-cut area. In all the conducted experiments (Experiments **I**, **II** and **III**), there was a significant decline in the water TN content and the decline was consistent at different scales, where the water volumes ranged from litres (Experiment **I** and **III**) to hundreds of litres (Experiment **II**). In all experiments, the TN content exhibited its steepest decline during the initial stages of the experiment when the biochar decreased the TN content in the water by 10 to 56% (from the initial content).

Previous studies have also demonstrated the potential of biochar to facilitate the retrieval of TN from different water sources (Dai et al., 2020). Adding biochar to constructed wetlands has been shown to improve the efficiency of inorganic N removal in domestic wastewater purification, increasing it from 46% to 68% when the initial N concentration in the incoming water was more than 50 mg L⁻¹ (Chand et al., 2022). Furthermore, Feng et al. (2022) demonstrated that the combination of biochar and constructed wetlands significantly improved the purification of synthetic wastewater; the addition of biochar resulted in removal rates of 92% for NH₄⁺-N, 90% for TN, and over 95% for heavy metals. Zheng et al. (2022) investigated the potential to utilise the biochar produced from sludge and cattail (*Typha latifolia*)-derived biochar as constructed wetland filling materials to enhance TN recovery from synthetic wastewater; TN removal using a constructed wetland without biochar was 67%, whereas the removal was enhanced to 91% when the sludge biochar was used, and to 81% when the cattail biochar was used. Zhou et al. (2019) also studied purification of domestic wastewater using constructed wetlands and reported that TN removal was improved from 10–39% to 21–50% by biochar addition.

In our study, the greatest adsorption capacity for TN was 0.19 mg g⁻¹ biochar (Table 4). Yin et al. (2017) reported a much higher adsorption capacity, where biochar adsorbed 0.7 to 140 mg inorganic N g⁻¹ biochar from the water. Experiments **I**, **II** and **III** revealed that the rather low adsorption capacity here was closely connected to the low initial N concentrations (Fig. 9). As the TN concentration in water increased, the adsorption of TN by both the spruce and birch biochar increased. The probable reason behind this phenomenon is the heightened concentration gradient of TN along the flow path, starting from the solution and extending towards the external surfaces, eventually reaching the inner biochar surfaces (Figure 8) (Largitte and Pasquier, 2016; Phuong Tran et al., 2022). Our results suggest that there is a threshold concentration below which adsorption of TN does not occur when natural runoff water is used. In our experiments, TN adsorption did not take place on the spruce biochar when the TN concentration in the runoff water was < 0.4 mg L⁻¹ (Experiment **II**), (Figure 9). The results here indicate that the performance of the biochar reactor was influenced by the initial TN concentration. Our findings align with the study conducted by Ahmadvand et al. (2018), who showed that an increase in the initial N concentration in the water corresponded to a higher level of N adsorption on the biochar.

Due to the low initial concentrations of NH₄⁺-N and P in the experiment described in Paper **I**, we were unable to determine the adsorption characteristics for NH₄⁺-N and P. During the initial five days of Experiment **II**, the concentrations of NO₃⁻-N and NH₄⁺-N decreased to levels below the detection limit, which was reflected in the high rate of TN removal at the beginning of the experiment. This occurrence can be attributed to the removal of mineral N

fractions from the runoff water. In addition, Experiment **II** clearly showed removal of dissolved organic N (Figure 10).

Multiple studies, including Wang et al. (2015), Takaya et al. (2016), Yin et al. (2017) and Wang et al. (2021) have provided evidence that support the efficacy of biochar as a viable adsorbent for $\text{NH}_4^+\text{-N}$. Nevertheless, in Experiment **I**, $\text{NH}_4^+\text{-N}$ was initially adsorbed by the biochar until its concentrations declined below the detection limit. It is important to note that a small fraction of $\text{NH}_4^+\text{-N}$ might have undergone reduction through volatilisation processes (Wu et al., 2021; Sha et al. 2019). Given the low concentrations of $\text{NH}_4^+\text{-N}$ in the runoff water, it is likely that the significance of the volatilisation process is minimal. The $\text{NH}_4^+\text{-N}$ concentration in the biochar columns (Experiment **II**) dropped rapidly at the beginning of the experiment. In comparison, the concentration of $\text{NH}_4^+\text{-N}$ began to increase after 15 days (Figure 10d). This could be due to a mechanism in which $\text{NO}_3^-\text{-N}$ substitutes $\text{NH}_4^+\text{-N}$ at the adsorption sites, or organic N degrades and releases $\text{NH}_4^+\text{-N}$. The increase in the flow velocity inside the column might also explain this process. In a study by Coleman et al. (2019), the addition of biochar (10–30% volume) to a woodchip reactor significantly improved the removal of $\text{NO}_3^-\text{-N}$ within 5 days. This enhancement was observed for representative $\text{NO}_3^-\text{-N}$ concentrations that are typically found in agricultural soil and ditch drains.

Usually, the biochar adsorption mechanism includes electrostatic attraction, ion exchange, ligand exchange, Lewis acid-base interaction and hydrogen bonds (Almanassra et al., 2021). In general, the $\text{NH}_4^+\text{-N}$ adsorption capacity of unmodified biochars derived from different biomass sources under different pyrolysis conditions is relatively low ($<20 \text{ mg g}^{-1}$ biochar) (Fan et al., 2019; Aghoghovwia et al., 2020). This adsorption is mainly driven by ion exchange and/or interactions with oxygen-containing functional groups on the biochar surfaces. The adsorption capacity of unmodified biochar is lower for $\text{NO}_3^-\text{-N}$, because a biochar surface that is mainly negatively charged reduces the adsorption of $\text{NO}_3^-\text{-N}$ by electrostatic repulsion (Zhang et al., 2020). The negatively charged surfaces of C-based particles (Yao et al., 2011) are expected to make biochar a poor adsorbent for anions. On the other hand, cations bound to the surface sites of biochar may boost anion adsorption on the layer of cations (Premarathna et al., 2019), thereby composing a diffuse double layer, as has been reported for clay minerals (Jeffrey et al. 2009). As shown in Experiments **I**, **II** and **III**, adsorption of $\text{NO}_3^-\text{-N}$ was observed, which would indicate that biochar is also capable of adsorbing anions. Biochar was able to decrease the $\text{NO}_3^-\text{-N}$ content in the water by between 5–55% from the initial content. These results are supported by the findings of Chintala et al. (2013), as well as Cai et al. (2016).

Previous research on the ability of biochar to absorb anions has shown inconsistent findings. Ion adsorption on the biochar surfaces is classified into four main categories: precipitation, chemical adsorption, physical adsorption and electrostatic adsorption (Fidel et al. 2018; Wang et al. 2022). The large surface area and porosity of biochar, as well as the presence of positively charged functional groups, are typically identified as the factors that determine the adsorption capability of $\text{NO}_3^-\text{-N}$ (Zhang et al. 2020; Fidel et al. 2018). The adsorption of $\text{NO}_3^-\text{-N}$ has been observed to increase with a rise in the biochar pyrolysis temperature and a lowering of pH, which is most likely related to an anion exchange adsorption process (Fidel et al. 2018). The presence of various functional groups, such as carboxylic, hydroxyl, lactone and ketone groups has been found to increase the adsorption of $\text{NO}_3^-\text{-N}$ (Chintala et al., 2013; Cai et al., 2016; Ahmadvand et al., 2018). Biochar may adsorb more $\text{NO}_3^-\text{-N}$ at a lower liquid pH, according to Chintala et al. (2013), since the biochar surfaces become more positively charged owing to the protonation process. Competitive

adsorption, on the other hand, reduces the adsorption of NO_3^- -N when the solution includes significant quantities of other anions (Chintala et al., 2013). Nonetheless, incapability or the limited ability of biochar to adsorb N compounds has also been observed (Zhang et al., 2020; Hollister et al. 2013). Only two out of thirteen varieties of biochar were found to be capable of adsorbing NO_3^- -N, according to Yao et al. (2012), while Gai et al. (2014) revealed that some NO_3^- -N was released from biochar. Different preparation procedures, the distinct properties of the biochar generated from different biomass, and different initial concentrations of N compounds in the solution might explain the inconsistencies between these observations.

4.2 Adsorption kinetics

Kinetic models offer valuable insights into the equilibrium state of adsorbent materials and adsorbates, thereby providing a comprehensive understanding of their interaction. The pseudo-first and pseudo-second-order kinetic models effectively captured the chemical adsorption processes between the adsorbate and adsorbent, and so provide crucial information with regard to the maximum adsorption capacity and adsorption rate (Zhao et al., 2018). Cheng et al. (2021) demonstrated that the pseudo-second-order kinetics model effectively describes the adsorption kinetics of compounds by biochar, which would suggest chemical adsorption behaviour associated with the biochar.

The design of a biochar reactor relies mainly on adsorption parameters because the mechanisms of adsorption are strongly influenced by kinetics and thermodynamics, regardless of the type of adsorbent or the nature of the contaminant. In both column experiments here and various operational systems associated with fluid dynamics and transfer phenomena (Asfaram et al., 2017), nonlinear models have shown greater efficacy in capturing experimental kinetics and isotherm data compared to linear models (Tran et al., 2016; Tran et al., 2017; Sheikholeslami et al., 2018). In the current research, both models performed similarly against the experimental data. In Experiment **III**, the maximum adsorption capacity at equilibrium (Q_{max}) increased with increasing TN content in the solution. Other studies have found that when the initial concentration of N increases, the maximum adsorption capacity also increases (Milmile et al., 2011; Olgun et al., 2013). The results of the kinetic models in Experiment **III** revealed that Q_{max1} (pseudo-first order model) was approximately three to four times, and Q_{max2} (pseudo-second order model) was nearly two times greater at TN concentrations of 4 mg L^{-1} than at 1 mg L^{-1} . The results obtained from Experiment **III** imply that birch biochar demonstrates a considerably greater Q_{max} value when compared to spruce biochar (Figure 8), which would support the observations made in Experiment **I**. In addition, the Q_{max} value exhibited an upward trend as TN concentrations increased, which can be attributed to the enhanced accessibility of N in the solution at higher initial N concentrations (Largitte & Pasquier, 2016).

In Experiment **I**, the adsorption rates were identical between the various biochar treatments. The most significant variation between the treatments was in the adsorption capacity. Q_{max} decreased as the biochar particle size increased, which might be because the surface area available for adsorption reduces as the particle size rises (Jin et al. 2022; Eberhardt and Min 2008). Despite the fact that spruce biochar had a greater specific surface area ($320 \text{ m}^2 \text{ g}^{-1}$) than birch biochar ($260 \text{ m}^2 \text{ g}^{-1}$), the latter exhibited a greater Q_{max} value. While increasing the surface area of biochar may enhance the adsorption of N (Zhang et al., 2012), adsorption capacity is not entirely reliant on the surface area of the biochar (Zhang et al., 2012; Zhang et al., 2014; Takaya et al., 2016).

When the pH of the water was elevated, the influence of biochar on water quality was obvious. The pH of water is a significant factor in determining the capacity of ion exchange and, consequently, the adsorption of N onto the surface of the biochar (Jin et al., 2022; Yin et al., 2017). The Q_{max} value of biochar exhibits a noticeable increase with an increase in the pH value in the solution (Yin et al., 2017). In our study, the initial pH of the water samples was found to be moderately acidic (~ 6), which aligns with the typical acidity observed in runoff waters that originate from boreal peatlands (Åström et al., 2001). Under low pH conditions, there is a potential for competition between H^+ and NH_4^+ ions for active sites on the surface of the biochar. This competition can limit the adsorption of N, as observed by Novak et al., (2010). Nevertheless, under basic conditions, NO_3^- -N is minimally adsorbed due to increased competition for adsorption sites on the surfaces of the biochar between the hydroxide ions (OH^-) and the NO_3^- -N ions (Chintala et al., 2013; Iida et al. 2013).

4.3 Desorption dynamics

In Experiment **I**, we found no evidence of N desorption from the biochar (215 hours). This was most likely due to the restricted amount of N in the water samples. In Experiment **III**, the release of TN from the birch biochar was significantly greater compared to the spruce biochar, which aligns with the greater adsorption capacity of birch biochar. Conversely, spruce biochar exhibited negative values for TN release, which would suggest adsorption rather than desorption of TN. This implies that spruce biochar was not fully saturated. The findings also indicate that as the TN concentration in the water increased, there was a corresponding increase in the amount of TN released from the birch biochar, which is in line with the findings of Chintala et al., (2013).

The desorption process involves several mechanisms, such as the presence of exchangeable ions in the water with limited bond energy, organic molecule entrapment within micropores and pore deformation mechanisms (Zhang et al., 2010; Chintala et al., 2013; Dechene et al., 2014). Zhu and Selim (2000) also discussed the distinctions between adsorption and desorption isotherms. Due to the temporal fluctuation in TN concentrations, the end use of biochar to eliminate N compounds from peatland runoff water might be difficult to anticipate. Despite the substantial TN adsorption capacity of birch biochar ($0.309 \text{ mg TN g biochar}^{-1}$), only a small portion (1.29% or $0.004 \text{ mg TN g biochar}^{-1}$) was released during the experiment reported in Experiment **III**. In contrast, spruce biochar exhibited a modest release ($\sim 0.9\%$ or $0.002 \text{ mg TN g biochar}^{-1}$) from the total amount of TN adsorbed ($0.208 \text{ mg TN g biochar}^{-1}$). These results emphasise the minimal TN desorption rate of both spruce and birch biochar, underscoring the potential of biochar as an effective solution to protect water quality. This becomes particularly relevant in regions where peatlands contribute significantly to nutrient discharge.

4.4 Biochar as a Water Protection Tool

Water protection is an important aspect of forest management that aims to reduce the negative human-induced impact of peatland forestry on water quality. Currently, a number of methods are used to reduce nutrient loading, to slow down discharge rates, and to facilitate sedimentation of suspended solids (Hägglom et al., 2020). Such methods include constructed wetlands, overland flow fields, sedimentation ponds, sedimentation pits and peak-flow management approaches (Nieminen et al., 2018; Nieminen et al., 2005b; Eskelinen

et al., 2015; Joensuu et al., 1999). Despite the effectiveness of sedimentation ponds in removing coarse-textured mineral soil particles from discharge waters, they are relatively inefficient in removing fine-textured materials and peat particles (Sallantausta et al., 1998). The effectiveness of ponds for sediment control can be adversely affected by several factors, in particular the degradation of the pond walls. Moreover, the high cost of pond construction, coupled with the need for frequent maintenance, can make them impractical in some situations. Furthermore, clear-cut areas and sites with elevated levels of suspended solids in upstream drainage water may require regular cleaning and maintenance of the ponds.

The water quality of drained peatlands can also be improved by buffer zones, which are comparatively inexpensive and require no maintenance (Laurén et al., 2007). Peatland buffer zones, in particular, have been found to retain inorganic N with varying effectiveness, ranging from 58–93% (Vikman et al. 2010). However, the implementation of such buffer zones requires vast areas and may not be practical for peatlands that are intensively drained (Eskelinen et al., 2015). The effectiveness of N retention depends on a large buffer area and low runoff volume, while a small buffer area combined with a high runoff volume will considerably reduce the N removal efficiency (Vikman et al., 2010). A substrate composed of biochar has the potential to improve the N recovery efficiency since it can adsorb inorganic and organic pollutants (El Barkaoui et al., 2023). As such, the addition of biochar could be an effective method to control nutrient leaching (Cheng et al., 2022; Zheng et al., 2022).

Since biological activities are temperature-dependent, biological water protection methods outside of the growing season become ineffective. Concentrations of NO_3^- -N, for example, increase outside of the growing season (Palviainen et al., 2015). A high adsorption capacity and a low desorption rate are required for successful use of biochar in water protection (Wang et al., 2020), and so an understanding of the adsorption-desorption behaviour of birch and spruce biochar is essential. The results in this thesis indicate that biochar can be a useful and effective water protection method to clean runoff water from clear-cut forests. Our studies demonstrated that biochar has the potential to adsorb anions, as evidenced by the adsorption of NO_3^- -N. However, we also observed lower levels of NO_3^- -N adsorption, which were attributed to the low N concentration in the runoff water. Notably, our research concentrated on the potential application of biochar in clear-cut drained peatland areas. In these areas, the pattern of nutrient export differs from that of agricultural and urban runoff water systems. It is worth noting that existing water protection methods employed in forested peatlands to date have been inadequate in removing NO_3^- -N from the runoff water (Joensuu et al., 2002; Liljaniemi et al., 2003). This is a particular concern given that the current physico-chemical and biological techniques developed for NO_3^- -N removal are associated with high costs and can generate considerable amounts of byproducts that are concentrated in waste streams, thereby exacerbating the environmental impact of these methods (Bhatnagar and Sillanpää, 2011). In the context of peatland forestry, cost-effectiveness of NO_3^- -N removal has a specific significance due to the low profit margins that are typically associated with forest production. Our research findings provide compelling evidence of the potential of biochar-based adsorption to reduce NO_3^- -N leaching from nutrient-rich peatlands. This approach gains further relevance in the post-clear-cutting period, when N exports tend to increase significantly.

5 CONCLUSION

Peatland management practices in Finland cause substantial nutrient export to water bodies and this export is expected to increase in the near future due to increasing areas of peatland forest regeneration. This thesis highlights the capacity of biochar to recover both organic and inorganic N from the peatland runoff waters, which are characterised by elevated levels of dissolved organic material. Furthermore, the findings in this thesis indicate that the adsorption process is conditional upon the N concentration in the water. The investigation indicated a positive association between the adsorption capacity and the initial N concentration, which would suggest that elevated rates of nutrient export could enhance adsorption efficacy. This finding holds practical significance in the context of biochar reactor operations in the field, where the N concentration fluctuates seasonally.

The results from this thesis would indicate that a brief water residence time inside a biochar reactor would be adequate for nutrient adsorption onto the biochar surfaces under field conditions. Conversely, the implementation of a biochar reactor may not provide advantages in field sites that are characterised by extremely low levels of inorganic N concentrations.

Although the biochars in this thesis exhibited remarkable efficacy in the adsorption of TN, desorption upon exposure to low TN concentrations only resulted in the release of a minor fraction of the adsorbed TN from the biochar, thereby signifying its potential as an effective water protection measure in regions where elevated nutrient loading from peatlands pose a risk to aquatic ecosystems. The observed negligible desorption rate of TN underscores the promise of biochar as a viable and environmentally sustainable approach to preserve water quality.

The use of appropriate water protection methods contributes to the preservation and increase of biodiversity in the receiving water bodies, by improving the quality of the runoff waters. Seasonal changes in nutrient concentrations highlight the need for an effective water protection tool in peatland forestry, which is why the use of biochar for adsorption-based nutrient removal seems to be efficient. The results presented in this thesis have led to a better understanding of how biochar functions as a water protection tool for forestry. As a result of this understanding, it is possible to plan new schemes for water protection in forestry.

REFERENCES

- Aghoghovwia MP, Hardie AG, Rozanov AB (2020) Characterisation, adsorption and desorption of ammonium and nitrate of biochar derived from different feedstocks. *Environ. Technol* 43(5): 774-787. <https://doi.org/10.1080/09593330.2020.1804466>
- Ahtikoski A, Hökkä H (2019) Intensive forest management—Does it pay off financially on drained peatlands? *Can J. For. Res* 49: 1101–1113. <https://doi.org/10.1139/cjfr-2019-0007>
- Ahmadvand M, Soltani J, Hashemi Garmdareh SE, Varavipour M (2018) The relationship between the characteristics of biochar produced at different temperatures and its impact on the uptake of NO₃. *Environmental Health Engineering and Management* 5(2): 67–75. <https://doi.org/10.15171/EHEM.2018.10>
- Almanassra IW, Mckay G, Kochkodan V, Atieh MA, Al-Ansari T (2021) A state of the art review on phosphate removal from water by biochars. *Chem. Eng. J* 409: 128211. <https://doi.org/10.1016/j.cej.2020.128211>
- Ambaye TG, Vaccari M, van Hullebusch ED, Amrane M, Artimi S (2021) Mechanisms and adsorption capacities of biochar for the removal of organic and inorganic pollutants from industrial wastewater. *Int. J. Environ. Sci. Technol* 18: 3273–3294. <https://doi.org/10.1007/s13762-020-03060-w>
- Asfaram A, Ghaedi M, Ahmadi Azqhandi MH, Goudarzi A, Hajati S (2017) Ultrasound-assisted binary adsorption of dyes onto Mn@ CuS/ZnS-NC-AC as a novel adsorbent: Application of chemometrics for optimization and modeling. *J. Ind. Eng. Chem* 54: 377–388. <https://doi.org/10.1016/j.jiec.2017.06.018>
- Åström M, Aaltonen EK, Koivusaari J (2001) Impact of ditching in a small forested catchment on concentrations of suspended material, organic carbon, hydrogen ions and metals in stream water. *Aquat Geochem* 7: 57–73. <https://doi.org/10.1023/A:1011337225681>
- Battas A, El Gaidoumi A, Ksakas A, Kherbeche A (2019) Adsorption study for the removal of nitrate from water using local clay. *The Scientific World Journal* 2019: 1–10. <https://doi.org/10.1155/2019/9529618>
- Beesley L, Moreno-Jiménez E, Gomez-Eyles JL, Harris E, Robinson B, Sizmur T (2011) A review of biochars' potential role in the remediation, revegetation and restoration of contaminated soils. *Environ. Pollut* 159(12): 3269–3282. <https://doi.org/10.1016/j.envpol.2011.07.023>
- Bhatnagar A, Sillanpää M (2011) A review of emerging adsorbents for nitrate removal from water. *Chemical Engineering Journal* 168(2): 493-504. <https://doi.org/10.1016/j.cej.2011.01.103>
- Bilotta GS, Brazier RE (2008) Understanding the influence of suspended solids on water quality and aquatic biota. *Water Res* 42(12): 2849–2861. <https://doi.org/10.1016/j.watres.2008.03.018>
- Cai Y, Qi H, Liu Y, He X (2016) Sorption/desorption behavior and mechanism of NH₄⁺ by biochar as a nitrogen fertilizer sustained-release material. *Journal of Agricultural and Food Chemistry* 64(24): 4958–4964. <https://doi.org/10.1021/acs.jafc.6b00109>
- Cai Y, Liu L, Tian H, Yang Z, Luo X (2019) Adsorption and Desorption Performance and Mechanism of Tetracycline Hydrochloride by Activated Carbon-Based Adsorbents Derived from Sugar Cane Bagasse Activated with ZnCl₂. *Molecules* 24(24): 4534. <https://doi.org/10.3390/molecules24244534>

- Chand N, Kumar K, Suthar S (2022) Enhanced wastewater nutrients removal in vertical subsurface flow constructed wetland: Effect of biochar addition and tidal flow operation. *Chemosphere* 286: 131742. <https://doi.org/10.1016/j.chemosphere.2021.131742>
- Cheng N, Wang B, Wu P, Lee X, Xing Y, Chen M, Gao B (2021) Adsorption of emerging contaminants from water and wastewater by modified biochar: A review. *Environmental Pollution* 273:116448. <https://doi.org/10.1016/j.envpol.2021.116448>
- Cheng R, Hou S, Wang J, Zhu H, Shutes B, Yan B (2022) Biochar-amended constructed wetlands for eutrophication control and microcystin (MC-LR) removal. *Chemosphere* 295:133830, <https://doi.org/10.1016/j.chemosphere.2022.133830>
- Chintala R, Mollinedo J, Schumacher TE, Papiernik ShK, Malo DD, Clay DE., Kumar S, Gulbrandson D (2013) Nitrate sorption and desorption in biochars from fast pyrolysis. *Microporous and Mesoporous Materials* 179: 250–257. <https://doi.org/10.1016/j.micromeso.2013.05.023>
- Coleman BSI, Easton ZM, Bock EM (2019) Biochar fails to enhance nutrient removal in woodchips bioreactor columns following saturation. *J. Environ. Manag* 232: 490–498. <https://doi.org/10.1016/j.jenvman.2018.11.074>
- Conley DJ, Paerl HW, Howarth RW, Boesch DF, Seitzinger SP, Havens KE, Lancelot C, Likens GE (2009) Controlling eutrophication: Nitrogen and phosphorus. *Science* 323(5917): 1014–1015. <http://dx.doi.org/10.1126/science.1167755>
- Dai Y, Wang W, Lu L, Yan L, Yu D (2020) Utilization of biochar for the removal of nitrogen and phosphorus. *Journal of Cleaner Production* 257: 120573, <https://doi.org/10.1016/j.jclepro.2020.120573>
- Dalahmeh SS (2016) Capacity of biochar filters for wastewater treatment in onsite systems—technical report. SLU report 2016:090. SLU—Swedish University of Agricultural Sciences, Uppsala (ISBN: 978-91-576-9398-3)
- Dechene A, Rosendahl I, Laabs V, Amelung W (2014) Sorption of polar herbicides and herbicide metabolites by biochar-amended soil. *Chemosphere* 109: 180–186. <https://doi.org/10.1016/j.chemosphere.2014.02.010>
- Eberhardt TL, Min SH (2008) Biosorbents prepared from wood particles treated with anionic polymer and iron salt: effect of particle size on phosphate adsorption. *Bioresour Technol* 99(3): 626–630. <https://doi.org/10.1016/j.biortech.2006.12.037>
- El Barkaoui S, Mandi L, Aziz F, Del Bubba M, Ouazzani N (2023) A critical review on using biochar as constructed wetland substrate: Characteristics, feedstock, design and pollutants removal mechanisms. *Ecological Engineering* 190: 106927. <https://doi.org/10.1016/j.ecoleng.2023.106927>
- Eskelinen R, Ronkanen AK, Marttila H, Kløve B (2015) Purification efficiency of a peatland-based treatment wetland during snow melt and runoff events. *Ecol. Eng* 84: 169–179. <https://doi.org/10.1016/j.ecoleng.2015.08.004>
- Fan R, Chen CL, Lin JY, Tzeng JH, Huang CP, Dong C, Huang CP (2019) Adsorption characteristics of ammonium ion onto hydrous biochars in dilute aqueous solutions. *Bioresour. Technol* 272: 465–472. <https://doi.org/10.1016/j.biortech.2018.10.064>
- Fawcett JK, Scott J (1960) A rapid and precise method for the determination of urea. *Journal of Clinical Pathology* 13(2): 156–159. <https://doi.org/10.1136/JCP.13.2.156>
- Feng K, He S, Zhao W, Ding J, Liu J, Zhao Q, Wei L (2022) Can biochar addition improve the sustainability of intermittent aerated constructed wetlands for treating wastewater containing heavy metals? *Chemical Engineering Journal* 444:136636, <https://doi.org/10.1016/j.cej.2022.136636>

- Fidel RB, Laird DA, Spokas KA (2018) Sorption of ammonium and nitrate to biochars is electrostatic and pH dependent. *Scientific Reports* 8: 17627. <https://doi.org/10.1038/s41598-018-35534-w>
- Finér L, Mattsson T, Joensuu S, Koivusalo H, Lauren A, Makkonen T, Nieminen M, Tattari S, Ahti E, Kortelainen P, Koskiahio J, Leinonen A, Nevalainen R, Piirainen S, Saarelainen J, Sarkkola S, Vuollekoski, M (2010) Metsäisten valuma-alueiden vesistökuormituksen laskenta. *Suomen ympäristö 10*. [A method for calculating nitrogen, phosphorus and sediment load from forest catchments. *Finnish Environment 10*.] [In Finnish.]
- Gai X, Wang H, Liu J, Zhai L, Liu S, Ren T, Liu H (2014) Effects of feedstock and pyrolysis temperature on biochar adsorption of ammonium and nitrate. *PLoS ONE* 9(12): e113888. <https://doi.org/10.1371/journal.pone.0113888>
- Gwenzi W, Chaukura N, Noubactep C, Mukome FND (2016) Biochar-based water treatment systems as a potential low-cost and sustainable technology for clean water provision. *J. Environ. Manag* 197: 732–749. <https://doi.org/10.1016/j.jenvman.2017.03.087>
- Häggbloom O, Härkönen L, Joensuu S, Keskisarja V, Äijö H (2020) Water management guidelines for agriculture and forestry. Ministry of Agriculture and Forestry of Finland 12. <http://urn.fi/URN:ISBN:978-952-366-381-7>
- Hahti K (2018) Modelling Hydrology and Sediment Transport in a Drained Peatland Forest. Focus on Sediment Load Generation and Control after Ditch Network Maintenance. Doctoral dissertations. Aalto University, Helsinki, Finland, ISSN 1799-4934, 45. p. 52.
- Hollister CC, Bisogni JJ, Lehmann J (2013) Ammonium, nitrate, and phosphate sorption to and solute leaching from biochars prepared from corn Stover (L.) and Oak Wood (spp.). *Journal of Environmental Quality* 42(1): 137–144. <https://doi.org/10.2134/jeq2012.0033>
- Hynninen A (2011) Use of wetland buffer areas to reduce nitrogen transport from forested catchments: Retention capacity, emissions of N₂O and CH₄ and vegetation composition dynamics. *Dissertations Forestales* 129. pp 53. <https://doi.org/10.14214/df.129>
- Hyvönen R, Olsson BA, Lundkvist H, Staaf H (2000) Decomposition and nutrient release from *Picea abies* (L.) Karst. and *Pinus sylvestris* L. logging residues. *For. Ecol. Manag* 126(2): 97–112. [https://doi.org/10.1016/S0378-1127\(99\)00092-4](https://doi.org/10.1016/S0378-1127(99)00092-4)
- Iida T, Amano Y, Machida M, Imazeki F (2013) Effect of surface property of activated carbon on adsorption of nitrate ion. *Chem Pharm Bull* 61(11): 1173–1177. <https://doi.org/10.1248/cpb.c13-00422>
- Inyang M, Dickenson E (2015) The potential role of biochar in the removal of organic and microbiological contaminants from potable and reuse water: A review. *Chemosphere* 134: 232–240. <https://doi.org/10.1016/j.chemosphere.2015.03.072>
- Jafari M, Rahimi MR, Ghaedi M, Javadian H, Asfaram A (2017) Fixed-bed column performances of azure-II and auramine-O adsorption by *Pinus eldarica* stalks activated carbon and its composite with zno nanoparticles: Optimization by response surface methodology based on central composite design. *J. Colloid Interface Sci* 507: 172–189. <https://doi.org/10.1016/j.jcis.2017.07.056>
- Jeffrey NM, Warren BJ, David LL, Mohamed A, Don W, Mohamed AS (2009) Impact of Biochar Amendment on Fertility of a Southeastern Coastal Plain Soil. *Soil Science* 174 (2): 105–112. <http://dx.doi.org/10.1097/SS.0b013e3181981d9a>

- Jin Zh, Xiao Sh, Dong H, Xiao H, Tian R, Chen J, Li Y, Li L (2022) Adsorption and catalytic degradation of organic contaminants by biochar: Overlooked role of biochar's particle size. *Journal of Hazardous Materials* 422: 126928. <https://doi.org/10.1016/j.jhazmat.2021.126928>
- Joensuu S, Ahti E, Vuollekoski M (1999) The effects of peatland forest ditch maintenance on suspended solids in runoff Boreal Environ. Res 4(4): 343–355.
- Joensuu S (2002) Effects of ditch network maintenance and sedimentation ponds on export loads of suspended solids and nutrients from peatland forests. Doctoral thesis, Finnish Forest Research Institute, Research Papers 868. 83 p.
- Joensuu S, Ahti E, Vuollekoski M (2002) Effects of ditch network maintenance on the chemistry of run-off water from peatland forests. *Scand. J. For. Res* 17: 238–247. <https://doi.org/10.1080/028275802753742909>
- Kearns JP, Wellborn LS, Summers RS, Knappe DRU (2014) 2,4-D adsorption to biochars: Effect of preparation conditions on equilibrium adsorption capacity and comparison with commercial activated carbon literature data. *Water Res* 62: 20–28. <https://doi.org/10.1016/j.watres.2014.05.023>
- Killham K (1994) *Soil Ecology*. Cambridge University Press, Cambridge. 242 pp. <https://doi.org/10.1017/9780511623363>
- Konneh M, Wandera SM, Murunga SI, Raude JM (2021) Adsorption and desorption of nutrients from abattoir wastewater: modelling and comparison of rice, coconut and coffee husk biochar. *Heliyon* 7(11): e08458. Published 2021 Nov 23. <https://doi.org/10.1016/j.heliyon.2021.e08458>
- Kreutzweiser DP, Hazlett PW, Gunn JM (2008) Logging impacts on the biogeochemistry of boreal forest soils and nutrient export to aquatic systems: A review. *Environ. Rev* 16: 157–179. <https://doi.org/10.1139/A08-006>
- Largitte L, Pasquier R (2016) A review of the kinetics adsorption models and their application to the adsorption of lead by an activated carbon. *Chemical Engineering Research and Design* 109: 495–504. <https://doi.org/10.1016/j.cherd.2016.02.006>
- Laurén A, Koivusalo H, Ahtikoski A, Kokkonen T, Finér L (2007) Water protection and buffer zones: How much does it cost to reduce nitrogen load in a forest cutting? *Scand. J. For. Res* 22: 537–544. <https://doi.org/10.1080/02827580701614487>
- Lehmann J, Joseph S (2015) *Biochar for Environmental Management: Science, Technology and Implementation*, 2nd. ed; Routledge: London, UK; p. 944.
- Likens GE, Bormann FH (1999) *Biogeochemistry of a forested ecosystem*, 2nd edn. Springer-Verlag, Berlin. 159 pp. <https://doi.org/10.1007/978-1-4614-7810-2>
- Liljaniemi P, Vuori KM, Tossavainen T, Kotanen J, Haapanen M, Lepistö A, Kenttämies KE (2003). Effectiveness of constructed overland flow areas in decreasing diffuse pollution from forest drainages. *Environ. Manag* 32: 602–613. <https://doi.org/10.1007/s00267-003-2927-4>
- Liu J, Jiang S, Chen D, Dai G, Wei D, Shu Y (2020) Activation of persulfate with biochar for degradation of bisphenol A in soil. *Chemical Engineering Journal* 381: 122637. <https://doi.org/10.1016/j.cej.2019.122637>
- Luke statistics database (2022). The amount of silvicultural and forest improvement work 1950- (ha) by year and type of work. Available online : https://statdb.luke.fi/PXWeb/pxweb/en/LUKE/LUKE_04%20Metsa_02%20Rakenn%20ja%20tuotanto_12%20Metsanhoito-%20ja%20metsanparannustyot/06a_tyomaarat_1950.px/table/tableViewLayout2/ (accessed on 16 June 2022).

- Lundin L (1999) Effects on hydrology and surface water chemistry of regeneration cuttings in peatland forests. *International Peat Journal* 9: 118–126.
- Marttila V, Granholm H, Laanikari J, Yrjölä T, Aalto A, Heikinheimo P, Honkatukia J, Järvinen H, Liski J, Merivirta R, Paunio M (2005) Finland's National Strategy for Adaptation to Climate Change. Ministry of Agriculture and Forestry of Finland Publication 1a/2005, 281p.
- Marttila H, Kløve, B (2009) Retention of sediment and nutrient loads with peak runoff control. *Journal of Irrigation and Drainage Engineering* 135: 210–216. [https://doi.org/10.1061/\(ASCE\)0733-9437\(2009\)135:2\(210\)](https://doi.org/10.1061/(ASCE)0733-9437(2009)135:2(210))
- Matero J (2004) Cost-effective measures for diffuse load abatement in forestry. *Silva Fennica* 38(3): 333–345. <https://doi.org/10.14214/sf.420>
- Mattson K G, Swank W T, Waide J B (1987) Decomposition of woody debris in a regenerating, clear-cut forest in the Southern Appalachians. *Can. J. For. Res* 17: 712–721. <https://doi.org/10.1139/x87-114>
- Mattsson T (2010) Export of organic matter, sulphate and base cations from boreal headwater catchments downstream to the coast: Impacts of land use and climate. *Monogr. Boreal Environ. Res* 36: 49.
- Mattsson T, Kortelainen P, Räike A, Lepistö A, Thomas DN (2015) Spatial and temporal variability of organic C and N concentrations and export from 30 boreal rivers induced by land use and climate. *Science of the Total Environment* 508: 145–154. <https://doi.org/10.1016/j.scitoenv.2014.11.091>
- Micromeritics Flowsrb II 2300 (1986) Micromeritics Instrument Corporation: Atlanta, GA, USA.
- Milmile SN, Pande JV, Karmakar S, Bansiwala A, Chakrabarti T, Biniwale, RB (2011) Equilibrium isotherm and kinetic modeling of the adsorption of nitrates by anion exchange Indion NSSR resin. *Desalination* 276 (1–3): 38–44. <https://doi.org/10.1016/j.desal.2011.03.015>
- Ministry of the Environment of Finland (2006) Finland's fourth national communication under the United Nations framework convention on climate change. <http://urn.fi/URN:NBN:fi:bib:me:I00305292201>
- Miranda KM, Espey MG, Wink DA (2001) A Rapid Simple Spectrophotometric Method for Simultaneous Detection of Nitrate and Nitrite. *Nitric Oxide* 5(1): 62–71. <https://doi.org/10.1006/niox.2000.0319>
- Mizuta K, Matsumoto T, Hatate Y, Nishihara K, Nakanishi T (2004) Removal of nitrate-nitrogen from drinking water using bamboo powder charcoal. *Biores Technol* 95: 255–257. <https://doi.org/10.1016/j.biortech.2004.02.015>
- Mohan D, Sarswat A, Ok YS, Pittman CU (2014) Organic and inorganic contaminants removal from water with biochar, a renewable low cost and sustainable adsorbent—a critical review. *Bioresour. Technol* 160: 191–202. <https://doi.org/10.1016/j.biortech.2014.01.120>
- Moussout H, Ahlafi H, Aazza M, Maghat H (2018) Critical of linear and nonlinear equations of pseudo-first order and pseudo-second order kinetic models. *Karbala Int. J. Mod. Sci* 4: 244–254. <https://doi.org/10.1016/j.kijoms.2018.04.001>
- Nieminen M (2003) Effects of clear-cutting and site preparation on water quality from a drained Scots pine mire in southern Finland. *Boreal Environ. Res* 8: 53–59.
- Nieminen M (2004) Export of dissolved organic carbon, nitrogen and phosphorus following clear-cutting of three Norway spruce forests growing on drained peatlands in southern Finland. *Silva Fenn* 38 (2): 123–132. <https://doi.org/10.14214/sf.422>

- Nieminen M, Ahti E, Nousiainen H, Joensuu S, Vuollekoski M (2005a) Does the use of riparian buffer zones in forest drainage sites to reduce the transport of solids simultaneously increase the export of solutes? *Boreal Environ. Res* 10: 191–201
- Nieminen M, Ahti E, Nousiainen H, Joensuu S, Vuollekoski M (2005b) Capacity of riparian buffer zones to reduce sediment concentrations in discharge from peatlands drained for forestry. *Silva Fennica* 39: 331–339. <https://doi.org/10.14214/sf.371>
- Nieminen M, Ahti E, Koivusalo H, Mattsson T, Sarkkola S, Laurén A (2010) Export of suspended solids and dissolved elements from peatland areas after ditch network maintenance in South-Central Finland. *Silva Fenn* 44 (1): 39–49. <https://doi.org/10.14214/sf.161>
- Nieminen M, Sallantausta T, Ukonmaanaho L, Nieminen T, Sarkkola S (2017) Nitrogen and phosphorus concentrations in discharge from drained peatland forests are increasing. *Sci Total Environ* 609: 974–981. <https://doi.org/10.1016/j.scitotenv.2017.07.210>
- Nieminen M, Piirainen S, Sikström U, Löfgren S, Marttila H, Sarkkola S, Laurén A, Finér L (2018) Ditch network maintenance in peat-dominated boreal forests: Review and analysis of water quality management options. *Ambio* 47: 535–545. <https://doi.org/10.1007/s13280-018-1047-6>
- Nieminen M, Launiainen S, Ojanen P, Sarkkola S, Laurén A (2020) Metsätalouden vesistökuormitus: nykykäsitys ja tulevaisuuden menetelmäkehitys. *Metsätieteen aikakauskirja vuosikerta 2020 artikkeli id 10336*. <https://doi.org/10.14214/ma.10336>
- Novak JM, Busscher WJ, Watts DW, Laird DA, Ahmedna MA, Niandou MAS (2010) Short-term CO₂ mineralization after additions of biochar and switchgrass to a Typic Kandiudult. *Geoderma* 154: 281–288. <https://doi.org/10.1016/j.geoderma.2009.10.014>
- Olgun A, Atar N, Wang S (2013) Batch and column studies of phosphate and nitrate adsorption on waste solids containing boron impurity. *Chemical Engineering Journal* 222: 108–119. <https://doi.org/10.1016/j.cej.2013.02.029>
- Oliveira RF, Patel AK, Jaisi DP, Adhikari S, Lu H, Khanal SK (2018) Review Environmental application of biochar Current status and perspectives. *Bioresour. Technol* 246: 110–122. <https://doi.org/10.1016/j.biortech.2017.08.122>
- Paavilainen E, Päivänen J (1995) Peatland forestry. *Ecological studies* 111. Springer-Verlag, Berlin, Heidelberg -New York. 248 p. ISBN 3-540-58252-5.
- Palviainen M, Finér L, Kurka AM, Mannerkoski H, Piirainen S, Starr M (2004) Decomposition and nutrient release from logging residues after clear-cutting of mixed boreal forest. *Plant Soil* 263: 53–67. <https://doi.org/10.1023/B:PLSO.0000047718.34805.fb>
- Palviainen M, Finér L, Laurén A, Launiainen S, Piirainen S, Mattsson T, Starr M (2014) Nitrogen, phosphorus, carbon, and suspended solids loads from forest clear-cutting and site preparation: Long-term paired catchment studies from Eastern Finland. *AMBIO* 43: 218–233. <https://doi.org/10.1007/s13280-013-0439-x>
- Palviainen M, Lehtoranta J, Ekholm P, Ruoho-Airola T, Kortelainen P (2015) Land Cover Controls the Export of Terminal Electron Acceptors from Boreal Catchments. *Ecosystems* 18: 343–358. <https://doi.org/10.1007/s10021-014-9832-y>
- Palviainen M, Berninger F, Bruckman VJ, Köster K, Assumpção CRM., Aaltonen H, Makita N, Mishra A, Kulmala L, Adamczyk B, Zhou X, Heinonsalo J, Köster E, Pumpanen J (2018) Effects of biochar on carbon and nitrogen fluxes in boreal forest soil. *Plant Soil* 425: 71–85. <https://doi.org/10.1007/s11104-018-3568-y>

- Päivänen J, Hånell B (2012) Peatland ecology and forestry — A sound approach. University of Helsinki Department of Forest Sciences Publications, 267p.
- Phuong Tran TC, Nguyen TP, Nguyen TT, Cuong Le P, Tran QB, Nguyen XC (2022) Equilibrium single and co-adsorption of nutrients from aqueous solution onto aluminium-modified biochar. *Case Studies in Chemical and Environmental Engineering* 5; 100181. <https://doi.org/10.1016/j.cscee.2022.100181>
- Pillai SB (2020) Adsorption in Water and Used Water Purification. In: Lahnsteiner, J. (eds) *Handbook of Water and Used Water Purification*. Springer, Cham. https://doi.org/10.1007/978-3-319-66382-1_4-1
- Premarathna KSD, Rajapaksha AU, Sarkar B, Kwon EE, Bhatnagar A, Ok YS, Vithanage M (2019) Biochar-based engineered composites for sorptive decontamination of water: A review. *Chemical Engineering Journal* 372: 536–550. <https://doi.org/10.1016/j.cej.2019.04.097>
- Rankinen K, Bernal JEC, Holmberg M, Vuorio K, Granlund K (2019) Identifying multiple stressors that influence eutrophication in a Finnish agricultural river. *Sci. Total Environ* 658: 1278–1292. <https://doi.org/10.1016/j.scitotenv.2018.12.294>
- Rosén K, Aronson JA, Eriksson HM (1996) Effects of clearcutting on stream water quality in forest catchments in central Sweden. *For. Ecol. Manag* 83: 237–244. [https://doi.org/10.1016/0378-1127\(96\)03718-8](https://doi.org/10.1016/0378-1127(96)03718-8)
- Sallantausta T, Vasander H, Laine J (1998) Metsätalouden vesistöhaittojen torjuminen ojitetuista soista muodostettujen puskurivyöhykkeiden avulla [Prevention of detrimental impacts of forestry operations on water bodies using buffer zones created from drained peatlands] *Suo* 49: 125–133, (In Finnish with English Summary).
- Sha Z, Li Q, Lv T, Misselbrook T, Liu X (2019) Response of ammonia volatilization to biochar addition: a meta-analysis. *Sci Tot Env* 655: 1387–1396. <https://doi.org/10.1016/j.scitotenv.2018.11.316>
- Sheikholeslami M, Jafaryar M, Bateni K, Ganji DD (2018) Two phase modeling of nanofluid flow in existence of melting heat transfer by means of HAM. *Indian J. Phys* 92: 205–214. <https://doi.org/10.1007/s12648-017-1090-3>
- Sikström U., Hökkä H (2016) Interactions between soil water conditions and forest stands in boreal forests with implications for ditch network maintenance. *Silva Fenn* 50(1): 1–29. <https://doi.org/10.14214/sf.1416>
- Sigh A, Nocerino J (2002) Robust estimation of mean and variance using environmental data sets with below detection limit observations. *Chemometrics and Intelligent Laboratory Systems* 60: 69–86, [https://doi.org/10.1016/S0169-7439\(01\)00186-1](https://doi.org/10.1016/S0169-7439(01)00186-1)
- Singh NB, Nagpal G, Agrawal S, Rachna (2018) Water purification by using Adsorbents: A Review. *Environmental Technology & Innovation* 11: 187–240. <https://doi.org/10.1016/j.eti.2018.05.006>
- Srinivasan P, Sarmah AK (2015) Characterisation of agricultural waste-derived biochars and their sorption potential for sulfamethoxazole in pasture soil: A spectroscopic investigation. *Sci. Total Environ* 502: 471–480. <https://doi.org/10.1016/j.scitotenv.2014.09.048>
- Stenberg L (2016) Erosion and sediment transport mechanism in drained peatland forest catchments after ditch network maintenance. Doctoral dissertation. Aalto University, 202.
- Takaya CA, Fletcher LA, Singh S, Anyikude KU, Ross AB (2016) Phosphate and ammonium sorption capacity of biochar and hydrochar from different wastes. *Chemosphere* 145: 518–527. <https://doi.org/10.1016/j.chemosphere.2015.11.052>

- Tamm CO (1991) Nitrogen in terrestrial ecosystems: Questions of productivity, vegetational changes, and ecosystem stability. *Ecological studies* 81, Berlin, Springer, 115 pp. <https://doi.org/10.1007/978-3-642-75168-4>
- Tran HN, You SJ, Chao HP (2016) Effect of pyrolysis temperatures and times on the adsorption of cadmium onto orange peel derived biochar. *Waste Manag. Res* 34: 129–138. <https://doi.org/10.1177/0734242X15615698>
- Tran HN, You SJ, Chao HP (2017) Fast and efficient adsorption of methylene green 5 on activated carbon prepared from new chemical activation method. *J. Environ. Manag* 188: 322–336. <https://doi.org/10.1016/j.jenvman.2016.12.003>
- Väänänen R, Nieminen M, Vuollekoski M, Nousiainen H, Sallantausta T, Tuittila ES, Ilvesniemi H (2008) Retention of phosphorus in peatland buffer zones at six forested catchments in southern Finland. *Silva Fennica* 42 (2): 211–231. <https://doi.org/10.14214/sf.253>
- Vikman A, Sarkkola S, Sallantausta T, Nousiainen H, Silvan N, Laine J, Nieminen M (2010) Nitrogen retention by peatland buffer zone areas in forested catchments in Finland. *Hydrobiologia* 641: 171–183. <https://doi.org/10.1007/s10750-009-0079-0>
- Wang C, Wang X, Li N, Tao J, Yan B, Cui X, Chen G (2022) Adsorption of Lead from Aqueous Solution by Biochar: A Review. *Clean Technol* 4: 629–652. <https://doi.org/10.3390/cleantechnol4030039>
- Wang T, Li G, Yang K, Zhang X, Wang K, Cai J, Zheng J (2021) Enhanced ammonium removal on biochar from a new forestry waste by ultrasonic activation: Characteristics, mechanisms and evaluation. *Science of The Total Environment* 778: 146295. <https://doi.org/10.1016/j.scitotenv.2021.146295>
- Wang D, Jiang P, Zhang H, Yuan W (2020) Biochar production and applications in agro and forestry systems: A review. *Science of The Total Environment* 723: 137775. <https://doi.org/10.1016/j.scitotenv.2020.137775>
- Wang S, Gao B, Zimmerman AR, Li Y, Ma L, Harris WG., Migliaccio KW (2015) Removal of arsenic by magnetic biochar prepared from pinewood and natural hematite. *Bioresource Technology* 175: 391–395. <https://doi.org/10.1016/j.biortech.2014.10.104>
- Wu D, Zhang Y, Dong G, Du Zh, Wu W, Chadwick D, Bol R (2021) The importance of ammonia volatilization in estimating the efficacy of nitrification inhibitors to reduce N₂O emissions: A global meta-analysis. *Environmental Pollution* 271: 116365. <https://doi.org/10.1016/j.envpol.2020.116365>
- Yao Y, Gao B, Inyang M, Zimmerman AR, Cao X, Pullammanappallil P, Yang L (2011) Removal of phosphate from aqueous solution by biochar derived from anaerobically digested sugar beet tailings. *Journal of Hazardous Materials* 190 (1–3): 501–507. <https://doi.org/10.1016/j.jhazmat.2011.03.083>
- Yao Y, Gao B, Zhang M, Inyang M, Zimmerman AR (2012) Effect of biochar amendment on sorption and leaching of nitrate, ammonium, and phosphate in a sandy soil. *Chemosphere* 89:1467–1471. <https://doi.org/10.1016/j.chemosphere.2012.06.002>
- Yin Q, Zhang B, Wang R, Zhao Z (2017). Biochar as an adsorbent for inorganic nitrogen and phosphorus removal from water: A review. *Environmental Science and Pollution Research* 24: 26297–26309. <https://doi.org/10.1007/s11356-017-0338-y>
- Yu L, Yu M, Lu X (2018) Combined application of biochar and nitrogen fertilizer benefits nitrogen retention in the rhizosphere of soybean by increasing microbial biomass but not altering microbial community structure. *Sci. Total Environ* 640–641: 1221–1230. <https://doi.org/10.1016/j.scitotenv.2018.06.018>

- Zhang H, Wang H, Gan J (2010) Effect of *Pinus radiata* derived biochars on soil sorption and desorption of phenanthrene. *Environmental Pollution* 158: 2821–2825. <https://doi.org/10.1016/j.envpol.2010.06.025>
- Zhang M, Gao B, Yao Y, Xue YW, Inyang M (2012) Synthesis of porous MgO-biochar nanocomposites for removal of phosphate and nitrate from aqueous solutions. *Chemical Engineering Journal* 210: 26–32. <https://doi.org/10.1016/j.cej.2012.08.052>
- Zhang Y, Li ZF, Mahmood IB (2014) Recovery of NH_4^+ by corn cob produced biochars and its potential application as soil conditioner. *Frontiers of Environmental Science & Engineering* 8: 825–834. <https://doi.org/10.1007/s11783-014-0682-9>
- Zhang M, Song G, Gelardi DL, Huang L, Khan E, Mašek O, Parikh SJ, Ok YS (2020) Evaluating biochar and its modifications for the removal of ammonium, nitrate, and phosphate in water. *Water Research* 186: 116303. <https://doi.org/10.1016/j.watres.2020.116303>
- Zhao H, Xue Y, Long L, Hu X (2018) Adsorption of nitrate onto biochar derived from agricultural residuals. *Water Science & Technology* 77(1–2): 548–554. <https://doi.org/10.2166/wst.2017.568>
- Zheng F, Fang J, Guo F, Yang X, Liu T, Chen M, Nie M, Chen Y (2022) Biochar based constructed wetland for secondary effluent treatment: Waste resource utilization, *Chemical Engineering Journal* 432: 134377. <https://doi.org/10.1016/j.cej.2021.134377>
- Zhou X, Wu S, Wang R, Wu H (2019) Nitrogen removal in response to the varying C/ N ratios in subsurface flow constructed wetland microcosms with biochar addition. *Environ. Sci. Pollut. Control Ser* 26(4): 3382–3391. <https://doi.org/10.1007/s11356-018-3871-4>
- Zhu H, Selim HM (2000) Hysteretic behavior of metolachlor adsorption–desorption in soils. *Soil Science* 165(8): 632–645. <https://doi.org/10.1097/00010694-200008000-00005>